UiT
THE ARCTIC UNIVERSITY OF NORWAY

FACULTY OF HEALTH SCIENCES
DEPARTMENT OF PHARMACY

Identifying signaling pathway responsible for SRC-3 serine 857 phosphorylation

A study in lung cancer cells

Gurjit Kaur
Master thesis in Pharmacy
May 2014

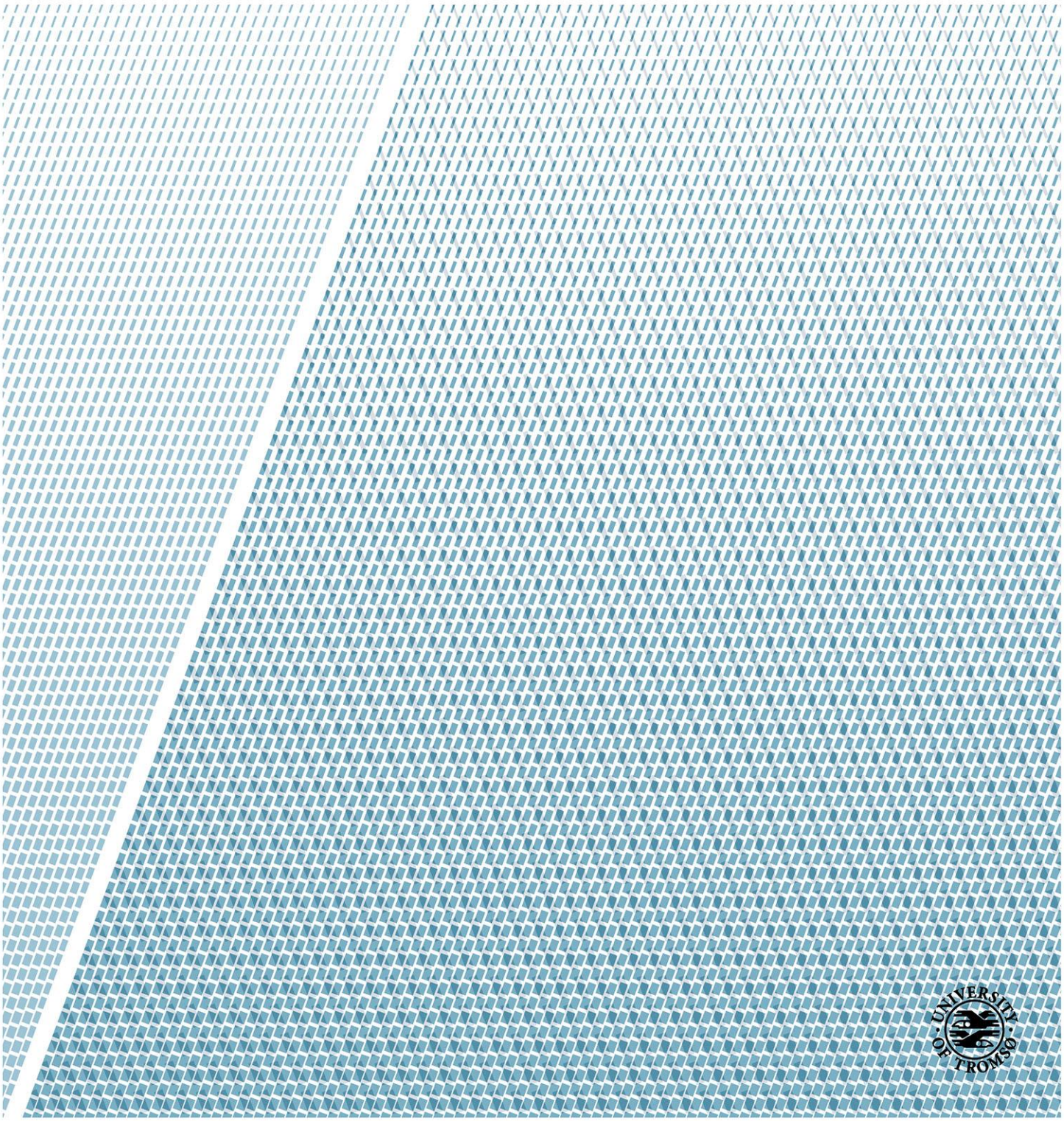

ACKNOWLEDGEMENTS

This work was carried out at the research group of Pharmacology at the Department of Pharmacy, University of Tromsø, from August 2013 – May 2014 under the supervision of Professor Ole Morten Seternes.

I would like to express my greatest appreciation to my supervisor Professor Ole Morten Seternes. Thank you for guiding me and for being so enthusiastic, especially every time I obtained results from the many western blot analysis I have run.

Everyone at the research group has been so kind and helped me through the work of this thesis. Thank you, Hanne Kildalsen, Bjarne Herold Johansen, Thomas Clemens Jensen, Espen Åberg and Rune Hogseth for your kind support and for answering all my (never-ending) questions. I have learned a lot thanks to your willingness to share your expertise with me.

Thank you, my fellow pharmacy students for being my family in Tromsø, far from home. I will miss all the good times we have had during our stay in North Norway. I would especially like to thank Limou Saba, Mahmoud Aburayya and Merete Kveli Moen for sharing happy moments of achieving good results as well as mishaps at the lab. What I will miss the most are the long lunch and tea/coffee breaks with Limou and our discussions constantly shifting from one topic to another.

Finally, I would like to thank mom and dad for always believing in me and my sisters. We are lucky to have you in our lives, and you have been so supportive and encouraging during our studies. The arrival of my adorable nephew, Viraj, has been a great distraction from my studies because of all the weekends of travelling south, but also a driving force for doing my best as I wish to be a role model for him. I look forward to see him more often in the future!

I dedicate this humble work to my family and all the wonderful people I have met in Tromsø.

Tromsø, May 2014

Gurjit Kaur

SUMMARY

Background: Signal transduction mediated by protein kinases and phosphatases is complex and highly coordinated. The mitogen activated protein kinases (MAPKs) are key components that transduce extracellular stimuli to biological responses by a three-tier module. The biological functions of steroid receptor coactivator-3 (SRC-3), a coactivator of nuclear hormone receptors and numerous transcription factors, is regulated by multiple pathways involving the MAP kinase signaling cascades. The oncogenic SRC-3 protein is found to be overexpressed in multiple human cancers, such as breast, prostate and lung cancer, and is implicated in the regulation of multiple physiological and pathological functions. The upstream kinase of SRC-3 phosphorylation at S857 *in vivo* has yet to be found, although ERK3 has been reported to phosphorylate this site.

Aim: In this study, we investigate the association of the ERK3-MK5 pathway with SRC-3 phosphorylation at S857 residue in the human lung cancer cells H1299.

Methods: *In vitro* and *in vivo* kinase assays, immunoprecipitation assays and western blot analysis.

Results: Unlike the MAPK kinases p38, ERK2 and ERK3, the MAPKAP kinases MK2 and MK5 phosphorylate SRC-3 at S857 efficiently *in vitro*. siRNA mediated knockdown of ERK3 and MK5 demonstrates no such effect *in vivo*. Blocking of the p38 MAPK pathway resulted in decreased levels of SRC-3 S857 phosphorylation compared to control, whereas stimulation with the stress-activator anisomycin significantly raised the phosphorylation levels *in vivo*.

Conclusion: In contrast to the study of Long et al, our results demonstrate the p38 MAPK pathway, rather than the ERK3-MK5 pathway, to be involved in the phosphorylation of SRC-3 at S857. Our observations should be further investigated to verify this association and to test if the phosphorylation is mediated through the MAPKAP kinase MK2.

Key words: Protein kinase, MAPKs, SRC-3, ERK3, p38, MK2, MK5, H1299 lung cancer cells

ABBREVIATIONS

AIB1	Amplified in breast cancer 1
AP-1	Activator protein-1
BSA	Bovine serum albumin
CID	CBP/p300 interacting domain
DMEM	Dulbecco's modified Eagle's medium
ER	Estrogen receptor
ERK	Extracellular signal-regulated kinase
FBS	Fetal bovine serum
GST	Glutathione S-transferase
IP	Immunoprecipitation
JNKs	c-Jun NH_2-terminal kinases
MAPK	Mitogen activated protein kinase
MAPKK	MAPK kinase
MAPKKK	MAPK kinase kinase
MEK	MAKPK/ERK kinase
MK2/5	MAPK-activated protein kinase 2/5
MMP	Matrix metalloproteinase
MSK	Mitogen- and stress-activated kinase
NES	Nuclear export sequence
NLK	Nemo-like kinase
NR	Nuclear hormone receptor

PBS	Phosphate buffered saline
PEA3	Polyomavirus enhancer activator 3
PKA	Protein kinase A
PR	Progesterone receptor
RPM	Rounds per minute
RSK	Ribosomal S6 kinase
RTK	Receptor tyrosine kinase
S857	Serine 857
SAPK	Stress-activated protein kinase
SDS-PAGE	Sodium dodecyl sulphate polyacrylamide gel electrophoresis
SRC	p160 steroid receptor coactivator
SRC-3	Steroid receptor coactivator-3
STAT	Signal transducer and activator of transcription
TF	Transcription factor
WB	Western blot
WCE	Whole cell extract
WT	Wild type

TABLE OF CONTENTS

LIST OF FIGURES

1 INTRODUCTION

Living cells monitor and respond to both their external and internal environment through signal transduction - a vital process carried out by complex and highly coordinated networks of proteins, which react to environmental changes. Binding of an impermeable signal molecule (ligand) to a receptor localized on the plasma membrane recognizing this specific ligand can result in the activation of an inherent enzymatic activity of the receptor, and thus stimulate one or more intracellular transducing proteins. The modulation of the protein(s) can eventually lead to the activation or inhibition of so called “effector proteins” involved in fundamental cellular processes such as apoptosis, differentiation, division, growth, metabolism, motility and transcription. Activity modulations of effector proteins can be effectuated by covalent modifications at the molecular level. Protein phosphorylation and de-phosphorylation, carried out by protein kinases and phosphatases respectively, are among the most common and important modifications (1, 2).

1.1 Protein kinases

Five hundred and eighteen protein kinase genes have been identified in the human genome (2). The protein kinases are enzymes that mediate most of the signal transduction in eukaryotic cells by modifying the substrate activity of other downstream proteins through covalently attaching phosphate to the side chain of serine, threonine or tyrosine. Thus, the protein kinases are divided into subgroups based on their catalytic specificity as tyrosine- or serine/threonine kinases. Some kinases have dual specificity and can phosphorylate both tyrosine and serine/threonine (3). The serine/threonine-specific kinases constitute approximately 80% of the protein kinases.

The balance of reversible protein phosphorylation is tightly regulated in order to maintain homeostasis, and also plays a critical role in intracellular processes during development, physiological responses and in functioning of the nervous and immune systems. Irregular phosphorylation results in, or is itself an outcome of, major diseases such as cancer, diabetes and rheumatoid arthritis (2, 4).Due to the role of protein kinases in a wide range of biological

processes mentioned above, they are attractive drug targets for the development of selective inhibitors, or possibly activators (2).

1.1.1 Tyrosine kinases

The tyrosine kinases (TKs) can be divided into two main groups: receptor TKs (RTKs) and non-receptor TKs. Non-RTKs are cytoplasmic proteins responsible for the transduction of extracellular signaling to downstream proteins, while the RTKs are membrane spanning cell surface receptors with a ligand-binding domain in the extracellular region, a single transmembrane helix, and a cytoplasmic region that contains the protein tyrosine kinase domain, in addition to carboxy terminal and juxtamembrane regulatory region. Upon ligand-binding, the RTKs will dimerize and autophosphorylate by catalyzing the transfer of the γ phosphate of ATP to hydroxyl groups of tyrosine groups on the receptors themselves and on target proteins. This is important for the transduction of extracellular signaling to the cytoplasm (5-7).

Through the phosphorylation of protein serine/threonine kinases, the RTKs activate various intracellular signaling pathways, including the phosphatiodylinositol-3 kinase/Akt (PI3K/Akt) pathway and the Raf-MEK-MAPK pathway (8). The latter pathway is of great interest and is widely investigated at many laboratories worldwide. This pathway is activated by RTKs binding to growth factors, such as epidermal growth factor (EGF), which lead to sequentially activation of the cascade Shc-Grb2-SOS-Ras-Raf-MEK-MAPK (9, 10).

1.1.2 Mitogen-activated protein kinases (MAPKs)

Fourteen genes in the human genome have been identified to code for mitogen-activated protein kinases. These kinases, expressed in all cell types, define 7 distinct signaling pathways (Figure 1) (11). The MAPKs regulate specific cellular responses to stimuli such as cytokines, growth factors, antigens, toxins and stress (temperature change, irradiation, and changes in cell shape, cell-cell interaction and extracellular matrix). The cellular responses differ from cell type to cell type (12).

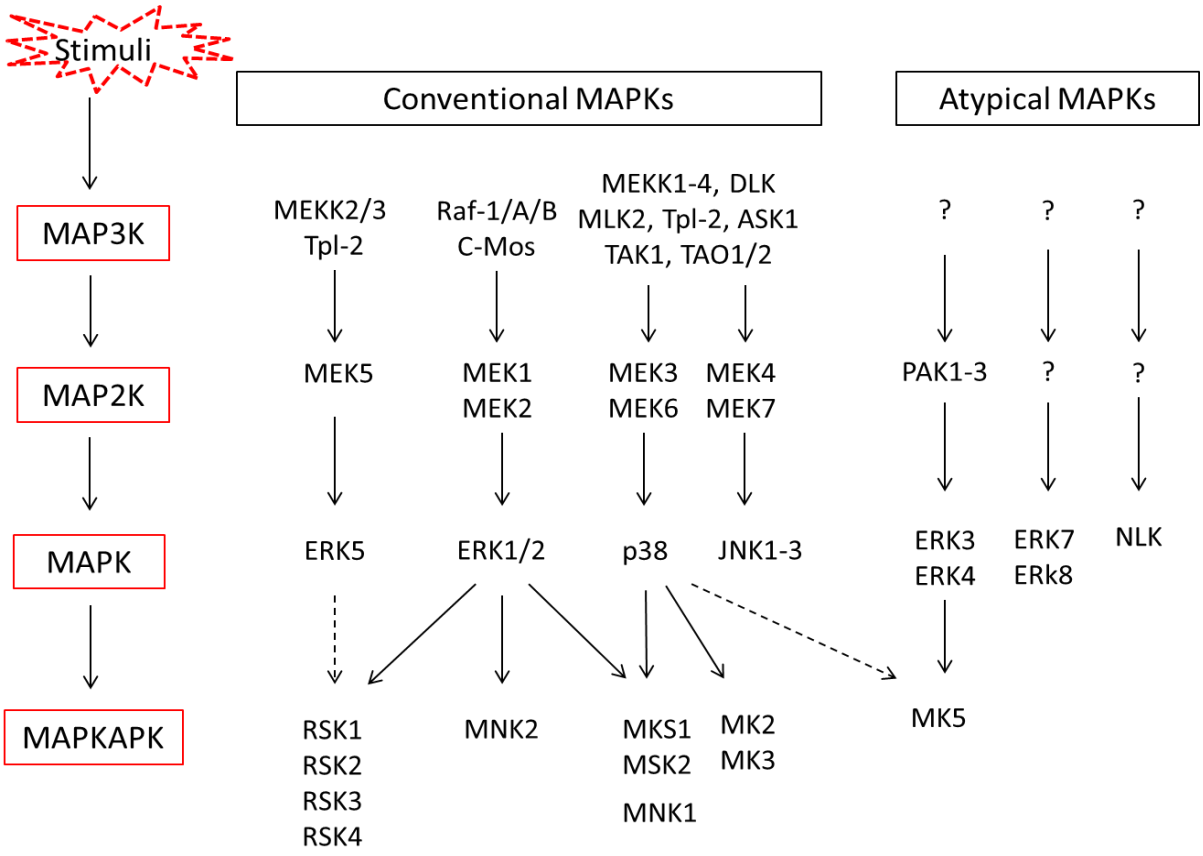

Figure 1: The MAPK signaling cascade of conventional and atypical MAPKs. The dotted lines indicate that the connection between the respective kinases remains to be fully elucidated. Figure is modified from Kostenko et al, 2012 (13).

The MAPKs are important intermediates in signal transduction pathways and are initiated by various cell surface receptors. They carry out signal transduction through a three-tier module - a cascade of phosphorylation at serine/threonine residues of the protein kinases. The MAPKs are activated by dual-specificity MAPK kinases (MAPKKs/MAP2Ks) by phosphorylation of both the threonine and tyrosine residues of a conserved T-X-Y motif within the activation loop of the MAP kinase. MAP2Ks are themselves phosphorylated and activated by MAPK

kinase kinases (MAPKKKs/MAP3Ks). The signals of the MAPK cascades can be amplifying by one successive protein in the cascade being more abundant than its regulator.

(12, 14, 15).

The MAPKs are evolutionary conserved and mainly phosphorylate serine and threonine residues which are next to proline rich residues. The docking domains of target substrates determine the specificity of the MAP kinases. By tethering the specific substrate to their docking motifs, the MAPKs help in the efficiency of the interactions. The phosphorylation reactions are regulated by various transcription factors (TFs) and enzymes, and further control of the interactions are mediated by other binding partners, subcellular localizations, conformational changes and protein stability (16).

The MAPKs are divided into two groups; the conventional kinases consisting of ERK1/ERK2, ERK5, JNKs and p38, and the atypical kinases comprising ERK3/ERK4, ERK7and NLK (11). The structural relationship of the conventional and atypical MAPKs is illustrated in Figure 2.

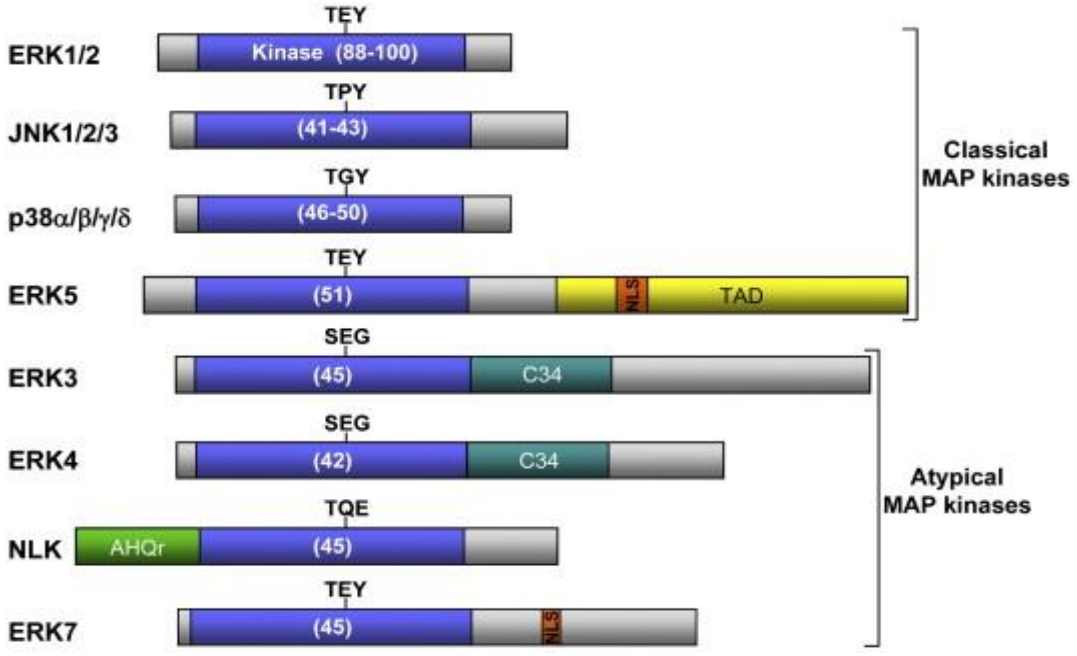

Figure 2: Schematic illustration of the structure of human MAPKs. Kinase domains (blue) with phosphorylation sites are shown along with nuclear localization sequence (NLS) and transactivation domain (TAD). C34: Conserved region in ERK3/4. AHQr: Ala/His/Gln-rich domain. Figure is adapted from Coulombe et al, 2007 (11).

1.1.2.1 Conventional kinases

ERK1/ERK2

Extracellular signal-regulated kinase 1 and 2 (ERK1/2, 43 and 41 kDa respectively) share 83% amino acid identity (17). These MAPKs are expressed to various extents in all tissues, and are activated upon phosphorylation within the conserved Thr-Glu-Tyr (TEY) motif in their activation loop by the dual specificity kinases MEK1/2 (18). MEK1/2 is activated by the kinase Raf, which is itself activated by Ras. Ras is activated by SOS (son of sevenless), which stimulates Ras to change GDP to GTP, allowing subsequent interaction with Raf. This cascade is often referred to as the Ras – Raf – MEK- ERK pathway and is among the most extensively studied pathway (19). The cascade is initiated by stimuli such as growth factors, cytokines, carcinogens and virus infections. Ligands for heterotrimeric guanine nucleotide-binding protein (G-protein) –coupled receptors and transforming agents are also activators of this pathway (20). When ERK1/2 is activated, significant amounts of the kinases accumulates in the nucleus where they activate nuclear substrates like the TFs SRC-1, Elk-1, c-Fos, c-Myc and STAT3. In addition, ERK1/2 phosphorylates substrates in other cellular compartments, e.g. membrane proteins (CD120a and calnexin) and cytoskeletal proteins (neurofilaments and paxillin). Several other substrates are activated by ERK1/2 as well; p90 ribosomal S6 kinase (RSK), mitogen and stress-activated kinase (MSK) and MAPK-interacting kinase (MNK) (18, 21).

ERK5

ERK5 (MAPK7) is ubiquitously expressed, but is especially found to be overexpressed in the heart, skeletal muscles, placenta, lungs and kidneys. The pathway of this conventional ERK plays an important role in embryogenesis, the development of the cardiovascular system and tumor neovascularization (22). It is activated by stress stimuli, cytokines, hormones, growth factors and neurotransmitters. It is phosphorylated by MEK5 on the residues Thr218 and Tyr220 within its conserved Thr-Glu-Tyr (TYE) motif in the activation loop (similar to ERK1/2). This kinase is also called BMK1 (Big MAPK1) due to a larger molecular mass than other ERKs due to a C-terminus extension, which regulates activation, autophosphorylation, subcellular localization and nuclear shuttling. Upon activation and autophosphorylation, ERK5 translocate to the nucleus where it phosphorylates and activates various TFs such as MEF2, Sap1, c-FOS and c-myc (16, 23).

JNKs

The c-Jun NH_2-terminal kinase (JNK) family of MAPKs is encoded by three genes; *Jnk1* and *2* which are ubiquitously expressed, and *Jnk3* whose expression is limited to the brain, heart and testis. Alternative splicing generates 10 distinct JNK isoforms which are involved in proliferation, apoptosis, motility, metabolism and DNA-repair. Together with p38, the JNKs constitute the stress-activated protein kinases (SAPKs).

Cytokines and environmental stress, such as UV radiation, growth factor deprivation, toxins and DNA-damaging agents, trigger the activation of MAP3Ks which phosphorylates and activates the two MAP2K isoforms MEK4 and MEK7. These two kinases will in turn phosphorylate and activate JNKs by dual phosphorylation of tyrosine and threonine residues at distinctive TPY motif. When JNKs are activated, they translocate from the cytoplasm to the nucleus where they phosphorylate distinct transcription factors, for example c-Jun which is a member of the activator protein-1 (AP-1) transcription factors (24-26).

p38

As mentioned above, p38 is a SAPK. p38 has four isoforms; α, β, γ (also called ERK6) and δ, which of p38α is the most well characterized (24). This group of MAPKs was discovered during a screen of drugs inhibiting TNF-α mediated inflammatory response (27). The p38 MAPK is characterized by the conserved Thr-Gly-Tyr (TGY) motif in its activation loop, which is phosphorylated by MEK3 and MEK6. MEK3 and MEK6 are activated by various MAP3Ks that are themselves activated by low molecular weight GTP-binding proteins from the Rho subfamily (e.g. Rac1, Cd242, Rho and Rit). The p38 pathway is induced by physical and chemical stresses, such as oxidative stress, hypoxia, x-ray and UV radiation and cytokines. In some instances, p38 is found to be activated by MEK4 (an activator of JNKs). Upon activation, p38 translocate from the cytosol to the nucleus where it phosphorylates Ser/Thr residues on its many substrates, amongst which MK2 is of great interest. The p38 pathway plays a role in the regulation of apoptosis, cell cycle progression, growth, differentiation, in the activation of p53 and may also be implicated in invasion and metastasis by its regulation of MMP2 and MMP9 (24, 28, 29).

1.1.2.2 Atypical kinases

ERK3/4

ERK3 and ERK4 are atypical MAP kinases with 44 % sequence homology to ERK1 and ERK2.There is major factors contributing to the distinction of the classical/conventional and atypical ERKs. First, ERK3 and ERK4 have a unique C-terminal extension which contributes to their larger size compared to ERK1 and ERK2. Second, ERK3 and ERK4 have a different motif in the activation loop compared to the conventional MAPKs; the canonical Thr-Xaa-Tyr (TXY) motif is replaced by a Ser-Glu-Gly (SEG) motif (Figure 2) (30).

ERK3 is found in both the nucleus and the cytoplasm, while ERK4 is mainly localized in the nucleus. Unlike ERK4, ERK3 is highly unstable with short half-life due to rapid degradation by ubiquitination via the 26S proteasome pathway (31, 32). MK5 is a downstream target of ERK3 and the phosphorylation of the key regulatory site Thr182 of MK5 by ERK3 leads to nuclear export of both the kinases. Increased levels of MK5 subsequently increases the activity of ERK3 by MK5 acting as a chaperone for ERK3 (15).

ERK7

ERK7 was first identified and characterized by Abe et al in 1999 (33). They reported that albeit ERK7 has the TEY motif, it is constitutive active, and that its c-terminal domain is required, rather than kinase activity, for its cellular localization and function as a negative regulator of growth. Very little information is obtained about its biological functions and its up- and downstream proteins since then. However, ERK7 has been shown to be a specific regulator of degradation of estrogen receptor alpha (ERα) through the 26S proteasome pathway in human breast cells (in which ERK7 is highly expressed). Loss of ERK7 has demonstrated to correlate with the progression of breast cancer (34).

NLK

Nemo-like kinase (NLK), a Ser/Thr kinase, is classified as an atypical kinase because of its N- and C-terminal extensions that are not present in the conventional MAPKs and because it has only a single residue in its activation loop which can be phosphorylated. NLK is activated by the Wnt pathway and by various cytokines (e.g. IL-6 and TGF-β), and it can regulate the Wnt pathway both positively and negatively (35).

1.1.3 MAPK-activated protein kinases (MAPKAPKs)

The MAPKAPK family has eleven family members that are generally activated by mitogens through the ERK1/2 kinase cascade (RSK1-4 and MNK2), stress stimuli through the p38 kinase cascade (MK2-3 and possibly MK5), or both of these cascades (MSK1-2 and MNK1) (see Figure 1) (18). Based on the homology of the kinase catalytic domain, the MAPKAPKs are considered to belong to the calcium/calmodulin-dependent protein kinase (CaMK) superfamily (36).

The RSKs and MSKs possess two distinct and functional kinase domains; the N-terminal kinase domain (NTKD) and the C-terminal kinase domain (CTKD). The MNKs, MK2-3 and MK5 have a single kinase domain homologous to the CTDK of the RSKs and MSKs. The activation loop sequences is similar in all of the MAPKAPKs and, as mentioned, is phosphorylated by either ERK1/2 or p38 MAP kinases. The RSKs are mainly involved in the regulation of gene expression, and its substrates for phosphorylation is, amongst others, Fos and cyclic-AMP-responsive-element binding protein (CREB). The MSKs are known to regulate gene expression by phosphorylating histone H3 (18, 36).

1.1.3.1 MAPK-activated protein kinase 2 (MK2)

MK2 is located in the nucleus and exist in an inactive, preformed complex with p38α that translocate to the cytoplasm upon activation. This translocation is initiated when p38 is activated by an upstream kinase (e.g. MEK3/6). MK2 is activated by p38 phosphorylating its three residues T221, S272 and T334. Maximal activation is obtained by the phosphorylation of any two of the sites, whereas phosphorylation of any one residue is in insufficient for its activation. Upon T334 phosphorylation, a nuclear export sequence (NES) of MK2 is unmasked and the complex of MK2-phospho p38 translocate from the nucleus to the cytosol. The NLS and NES are located in distinct regions of the C-terminus of MK2 and MK3, whereas these two signals are overlapping in MK5 (4, 36).

MK2 is found to regulate lipopolysaccharide (LPS-) induced up-regulation of several cytokine mRNAs, e.g. those encoding tumor necrosis factor and interleukin 6 and 8. The small heat shock protein Hsp27 is also phosphorylated by MK2, which modifies the ability of Hsp27 to act as a chaperone and thereby stabilize actin filament and regulate the cytoskeletal architecture. Finally, MK2 is also involved in the cell-cycle control at the CDC25- and p53-dependent checkpoints (31, 36).

1.1.3.2 MAPK-activated protein kinase 5 (MK5)

MK5 was originally identified as a p38-regulated/activated protein kinase (hence it is also called PRAK). Since then, it has been discovered not to be a direct downstream target of p38 and it does not act as a chaperone for p38 *in vivo* (31, 32). This kinase has two isoform that differs in two amino acids in MK5's unique C-terminal extension (36). The activation of MK5 is reported to be dependent on both ERK3 and ERK4, and these two MAP kinases are found to be physiological regulators of MK5 activity (31).

1.2 Protein kinase A (PKA)

The protein kinase A (PKA) is a tetramer consisting of a dimeric regulatory subunit (R2) and two monomeric catalytic subunits (C2), and has at least two isoforms. The type I isoform is mainly found in the cytoplasm, and the type II isoform is primarily associated with membranes, subcellular organelles and the cytoskeleton. The PKA pathway is stimulated by ligands binding to a G protein-coupled receptor (GPCR), which leads to increased cAMP levels. When cAMP bind to the R subunit of PKA, the catalytic subunits dissociates and become active. The free catalytic can then phosphorylate Ser and Thr residues which enables entrance into the nucleus and allow further phosphorylation of TFs, such as CREB, NF-κB and nuclear receptors. PKA modifies and influences the outcome of receptor activation by cross-talk with other pathways and is especially important in cellular differentiation and proliferation (37).

1.3 Steroid receptor coactivator-3

The p160 steroid receptor co-activator (SRC) family is a co-activator group consisting of three members: SRC-1/Nuclear receptor coactivator-1 (NCOA1), SRC-2/NCOA2/ TIF2/GRIP1 and SRC-3. SRC-3 was discovered in 1997 and is also known as Amplified In Breast cancer 1 (AIB1), NCOA3, Receptor Associated Coactivator-3 (RAC3), and p300/CBP interacting protein (CIP) (38).

The SRC-3 gene is localized in the chromosomal region 20q12 and the SRC-3 protein is a relatively large protein with its 160 kDa (39). Figure 3 illustrates the structural domains of SRC-3 of which three are considered to be basic structural domains analogues to the other SRC family members. First is the N-terminal basic helix-loop-helix-Per/ARNT/Sim domain (bHLH-PAS), which is the most highly conserved domain and is necessary for the interactions of SRC-3 with other DNA-binding proteins. Second is the receptor-interaction domain (RID) with its three LXXL motifs (L= leucine, X= any amino acid) by which SRC-3 binds to the ligand-activated nuclear receptors. Third is the C-terminal domain containing two intrinsic transcriptional activation domains; AD1 and AD2. AD1 interacts with histone aetyltransferases, and AD1 interacts with methyltransferases (39, 40).

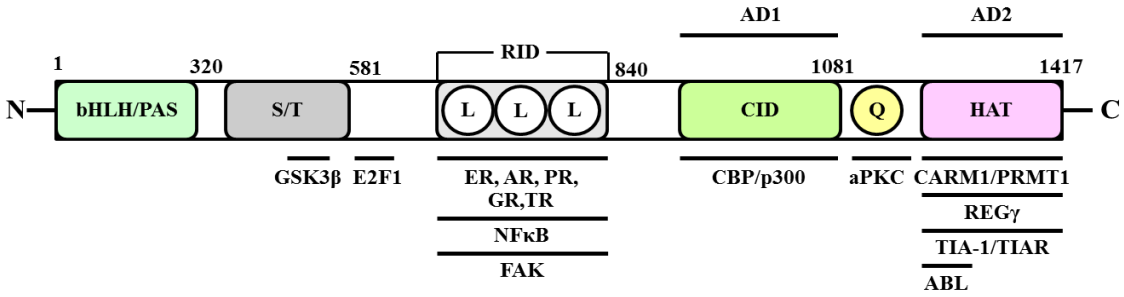

Figure 3: Structural domains of SRC-3 and its interacting partners. Illustration (not to scale) of conserved functional domains of SRC-3including bHLH/PAS (basic helix-loop-helix/per/ARNT/Sim homologous domain), S/T (serine/threonine) rich domain, a nuclear receptor interacting domain (RID) where L=LXXLL, the CBP/p300 interaction domain (CID), a polyglutamate region (Q), and a histoneacetyltransferase (HAT) domain. AD: activation domain. ER: estrogen receptor. AR: androgen receptor. PR: progesterone receptor. GR: glucocorticoid receptor. TR: thyroid receptor. aPKC: atypical protein kinase C. FAK: focal adhesion kinase. Figure is modified from York and O'Malley, 2010 (40).

The SRC-3 protein mediates transcriptional activities of nuclear hormone receptors (NRs) such as thyroid receptors, estrogen receptors (ER) and progesterone receptors (PR). The NRs are ligand-dependent transcription factors (TFs) which translocate to the nucleus when bound to its ligand. The ligand-NR complex recognizes specific DNA sequences and activates gene transcription after binding to its response elements upstream of target genes. The

transcriptional activation is optimized by interaction of hormone-activated NRs with co-activator proteins. This leads to an assembly and stabilization of a pre-initiation complex that conducts target gene transcription (38, 41).

SRC-3 also potentiates activities of several TFs, such as AP-1, E2F-1, nuclear factor κB (NF-κB), PEA3, and Signal Transducer and Activator of Transcription (STAT) (38). When the TFs binds to SRC-3, other chromatin modification factors, such as acetyltransferases (CBP and p300) and methyltransferases (CARM1 and PRMT1), are recruited. This results in modification of chromatin structure and activation of transcription of their target genes. Changes in concentration or activity of SRC-3 may result in altered expression level of many genes, and thereby influence a variety of cellular processes (42). The association of some of the interaction partners of SRC-3 and their tumor promoting properties are illustrated below.

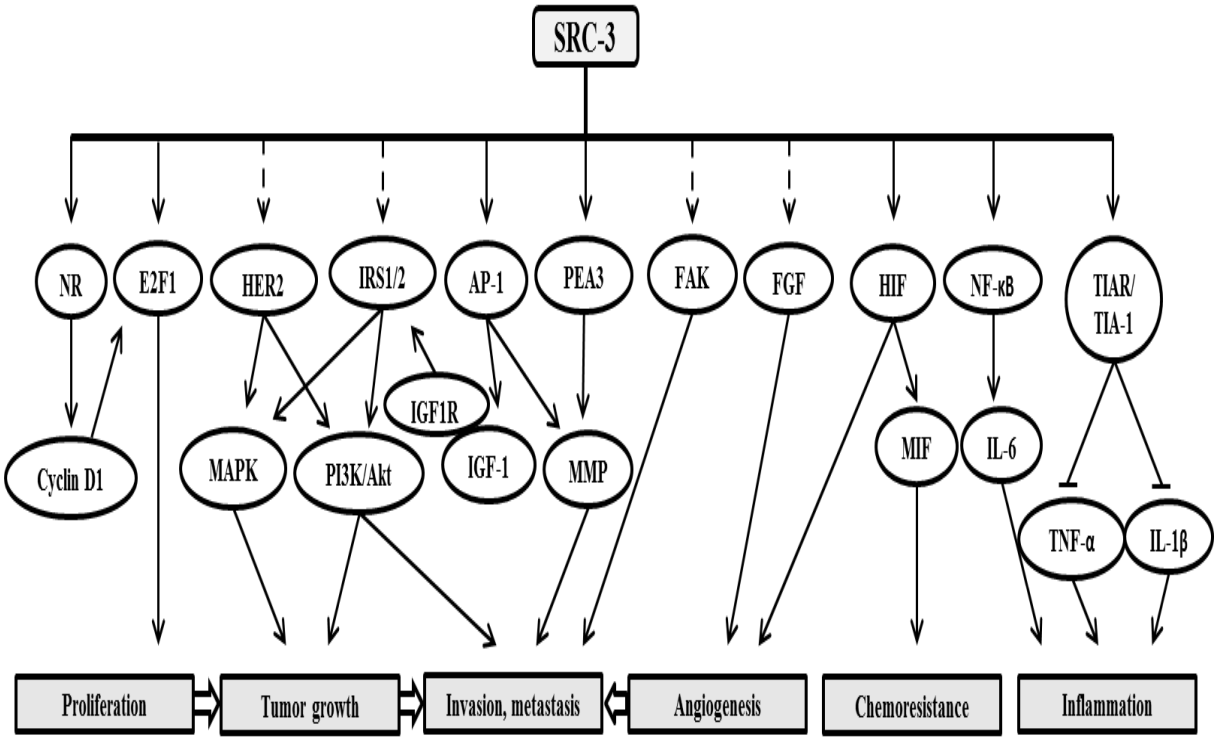

Figure 4: SRC-3 is implicated in multiple signaling pathways. SRC-3 promotes multiple hallmarks of cancer by its ability to coactivate various nuclear receptors and transcription factors. Direct interactions are illustrated by solid lines, whereas the dotted lines indicate indirect interaction. Figure is modified from Tien and Xu, 2012 (38).

2 AIM OF THESIS

A recent study by Long et al has shown that SRC-3 is a substrate of the atypical MAP-kinase ERK3 (43). They report the phosphorylation of SRC-3 by ERK3 to be specific for the residue Ser-857 (S857), and this phosphorylation was discovered to be important for the induction of MMP2, 9 and 10 expression, and thereby metastasis of lung cancer cells. The pharmacology research group of Tromsø has repeated some of these experiments, but with different outcome: SRC-3 appear to be a greater substrate of MK5 *in vitro*, rather than of ERK3. Like ERK3, MK5 is found to regulate expression of MMP2, 9 and 10. The research group has also found MK5 to be a downstream target and effector of ERK3, and the activation of MK5 to be associated with its phosphorylation at Thr-182 by ERK3 (32).

Considering this information, we wish to further investigate SRC-3 as a downstream target for the ERK3-MK5 pathway in the human lung cancer cells H1299 by addressing the following questions:

- Does ERK3 phosphorylate SRC-3 at S857 *in vitro* and/or *in vivo*?
- Does MK5 phosphorylate SRC-3 at S857 *in vitro* and/or *in vivo*?
- Does co-transfected ERK3 and SRC-3 bind *in vivo*, and how will the phosphorylation of SRC-3 at S857 be influenced by co-transfection of ERK3 and SRC-3?
- How will siRNA-mediated knockdown of MK5 and ERK3 influence phosphorylation of SRC-3 at S857?
- If the ERK3-MK5 pathway is not involved in the phosphorylation of SRC-3 at S857 *in vitro* and/or *in vivo*, are there alternative pathway(s) involved?

3 MATERIALS

Vectors

Plasmid	Catalog #	Source
pCMV Tag2B SRC-3 R:1.9 780ng/µl 28.10.13		Kindly provided by professor Gunnar Mellgren, University of Bergen

Proteins

Recombinant proteins	Catalog #	Source
Active-ERK2		Division of Signal Transduction Therapy (DSTT), University of Dundee, UK
Active-GSTMK2		
Active-MK5		
Active-GSTp38		
ERK3		Pharmacology research group, University of Tromsø
MEK inhibitor PD 184.352	Catalog # ALX-270-471	Alexis Biochemicals
p38 inhibitor SB-202190	Catalog # BML-EI294-0001	
PKA inhibitor H-89		Kindly provided by professor Richard Engh, University of Tromsø
SiRNA MK5 MAPKAPK5 20 nmole	Catalog # 16706	Ambion®
Scrambled SiRNA MK5 Negative Control siRNA #1 40 nmole	Catalog # AM46	
SiRNA ERK3 MAPK6 Silencer® validated siRNA 20 nmole	Catalog # AM553133	
Anisomycin		Sigma-Alderich®, St. Louis, MO, U.S.A.
EGF		

Plasmid purification kits

QIAGEN® Plasmid *Plus* Midi Kit	Catalog # 12945	QIAGEN®, Gmbh Hilden, Germany

Bacterial strains

E. Coli, DH5α competent cells	Pharmacology research group, University of Tromsø

Growth culture for bacteria

Ampicillin Sodium salt	Catalog # A9518	Sigma-Alderich®, St. Louis, MO, U.S.A.
LB-broth	10 g/l Bacto™ tryptone, Difco 5 g/l Bacto™ yeast extract, Difco 5 g/l NaCl pH adjusted to 7.4	SUMP section, University hospital in Northern Norway (UNN), Tromsø
LB-agar plate, 100µg/ml Ampicillin	10 g/l Bacto™ tryptone, Difco 5 g/l Bacto™ yeast extract, Difco 5 g/l NaCl pH adjusted to 7.4 10 g/l agar Ampicillin Sodium Salt, Sigma-Alderich®	
S.O.C. medium	20 g/l Bacto™ tryptone, Difco 5 g/l Bacto™ yeast extract, Difco 8.6 mM NaCl 2.5 mM KCL 10 mM MgCl 10 mM $MgSO_4$ 20 mM Glucose pH adjusted to 7.4	

Cell line

H1299	Carcinomic human non-small cell cancer, lung	LGG standards	ATCC® Number: CRL-5803™

Cell culturing medium

Dulbecco's Modified Eagle Medium (DMEM)	Catalog # D5796	Sigma-Alderich®, St. Louis, MO, U.S.A.

Cell transfection kits

Lipofectamine® 2000 Transfection Reagent	Catalog # 11668-019	Invitrogen, Life Technologies™, Carlsbad, CA, U.S.A.
Lipofectamine® LTX with Plus Reagent	Catalog # 15338-100	

Buffers, solutions and chemical reagents

Method		Composition/Catalog #	Source
Cell culturing	Dulbecco's Phosphate Buffered Saline (PBS)	Catalog # D8537	Sigma-Alderich®, St. Louis, MO, U.S.A.
	0.25% Trypsin-EDTA solution	Catalog # T4049	
	Penicillin-Streptomycin (10000 U/ml – 10 mg/ml)	Catalog # P0781	
	Fetal Bovine Serum (FBS) Superior	Catalog # S 0615	Biochrom AG®, Berlin, Germany
Cell transfection	Opti-MEM® I Reduced Serum Medium	Catalog # 11058-21	Gibco®, Life Technologies™, Carlsbad, CA, U.S.A.

Buffers, solutions and chemical reagents (continued)

Method		Composition/Catalog #	Source
Cell lysis & IP	SRC-3 lysis buffer	50 mM Tris [pH 7.5] 150 mM NaCl 0.5% Igepal 10 mM NaF 1 mM EDTA 1 mM EGTA 1 mM sodium orthovandate 10 mM β-glycerophosphate 5 mM NaPPi Milli-Q water ad 100 ml (1 tablet Complete, Mini, Protease inhibitor cocktail per 10 ml lysis buffer)	Pharmacology research group, University of Tromsø
	HA-lysis buffer	50 mM Tris [pH 7.5] 150 mM NaCl 2 mM EDTA 1 mM EGTA 1% Triton X-100 5 mM NaPPi 50 mM NaF 1 mM VO_4^{2-} 10 mM β-glycerophosphate Milli-Q water ad 100 ml (1 tablet Complete, Mini, Protease inhibitor cocktail per 10 ml lysis buffer)	
	MKK lysis buffer	20 mM Tris [pH 7.5] 1% TritonX-100 5 mM NaPPi 50 mM NaF 1mM EDTA 1mM EGTA 1 mM VO_4^{2-} 0,27 M sucrose 10 mM β-glycerophosphate Milli-Q water ad 100 ml	
	RIPA lysis buffer	50 mM Tris [pH 7.5] 150 mM NaCl 1% Sodium deoxycholate 1% Igepal 0.02% SDS 5 mM NaPPi 50 mM NaF 1 mM VO_4^{2-} 10 mM β-glycerophosphate Milli-Q water ad 100 ml (1 tablet Complete, Mini, Protease inhibitor cocktail per 10 ml lysis buffer)	

Buffers, solutions and chemical reagents (continued)

Method		Composition/Catalog #	Source
Cell lysis & IP	Complete, Mini, Protease inhibitor cocktail tablets	Catalog # 11836153001	Roche Diagnostics GmbH, Mannheim, Germany
	Anti-FLAG® M2 Magnetic Beads	Catalog # M8823	Sigma-Alderich®, St. Louis, MO, U.S.A.
	PureProteome™ Protein G Magnetic Bead System	Catalog # LSKMAGG10	©EMD Millipore Corporation, Billerica, MA, U.S.A.
	Blotting buffer	29 g Tris base 144 g glycerin 1 L methanol dH_2O ad 5 L	Pharmacology research group, University of Tromsø
SDS-PAGE/ Western blot	TBS buffer 10x	200 ml Tris 1M [pH 7.5] 400 g NaCl 10 g KCl dH_2O ad 5 L	Pharmacology research group, University of Tromsø
	TBS-T buffer 1x	200 ml Tris 1M [pH 7.5] 400 g NaCl 10 g KCl dH_2O ad 5 L	Invitrogen, Life Technologies™, Carlsbad, CA, U.S.A.
	NuPAGE® LDS Sample Buffer (4X)	Catalog # NP0008	
	NuPAGE® Sample Reducing Agent (10X)	Catalog # NP0009	
	NuPAGE® MES SDS Running Buffer (20X)	Catalog # NP0002-02	
	NuPAGE® Novex® 4-12 % Bis-Tris Protein Gels 1.0mm	Catalog # NP0321BOX	
	SeeBlue® Plus2 Pre-Stained Standard	Catalog # LC5925	

Buffers, solutions and chemical reagents (continued)

Method		Composition/Catalog #	Source
SDS-PAGE/ Western blot	Odyssey® Nitrocellulose Membrane	Catalog # P/N 926-31092	LI-COR Biosciences Odyssey, Lincoln, NE, U.S.A.
	Odyssey® Blocking buffer	Catalog # P/N 927-40000	
	Tween® 20	Catalog # P1379	Sigma-Alderich®, St. Louis, MO, U.S.A.
Kinase assay	Assay buffer	50 mM Tris-HCL 0,1 mM EGTA 1 mM sodium vandate 1 mM DTT dH_2O ad 1 ml	Pharmacology research group, University of Tromsø
	ATP-mix	3 % (v/v) 10 mM ATP 5 % (v/v) 1 M $MgCl_2$ 92 % Assay buffer	
	Kinase buffer (2 x)	100 mM Tris 0,2 mM EGTA 20 mM Magnesium acetate 200 µM ATP Milli-Q water ad 10 ml	
	Dilution buffer	50 mM Tris 1mg/ml BSA Milli-Q water ad 1 ml	

Antibodies

Primary antibodies	Source	Secondary antibodies	Source
SRC-3 (NCOA-3) Phos S857, 0,3 mg/ml 2nd bleed **Anti p-S857 SRC-3** (1:2000)	Custom made, Division of Signal Transduction Therapy (DSTT), University of Dundee, UK	Anti-Sheep IgG (H&L) Donkey IRDye 800CW P/N 613 732 168 (1:10000)	Rockland™ Immunochemical, Gilbertsville, PA, U.S.A.
GST (Z-5) Rabbit polyclonal IgG 200 µg/ml Catalog # sc-459 **GST-antibody** (1:200-1000)	Santa Cruz Biotechnology, Inc. Santa Cruz, CA, U.S.A.	Donkey anti-Rabbit IRDye® 680 LT 0,5 mg Catalog # 926-68023 (1:10 000)	LI-COR Biosciences Odyssey, Lincoln, NE, U.S.A.
NCoA-3 (M-397) Rabbit polyclonal IgG 200 µg/ml Catalog # sc-9119 **Anti SRC-3**(1:1000)	Santa Cruz Biotechnology, Inc. Santa Cruz, CA, U.S.A.		
ERK 2 (C-14) Rabbit polyclonal IgG 200 µg/ml Catalog # sc-154 **Anti ERK2** (1:1000)	Santa Cruz Biotechnology, Inc. Santa Cruz, CA, U.S.A.		
Pan-Actin Antibody Catalog # 4968 **Anti actin** (1:1000)	Cell signaling Technology, Inc.Danvers, MA U.S.A.		
Anti-FLAG® M2 Antibody Murine monoclonal IgG, 200 µg, 2 mg/ml Catalog # 200470-21 **Anti Flag M2** (1:1000)	Stratagene® Agilent Technologies, Inc	Donkey anti-Mouse IRDye® 800CW 0,5 mg Catalog # 926-32212 (1:10 000)	LI-COR Biosciences Odyssey, Lincoln, NE, U.S.A.
P-p44/42 MAPK (T202/Y204) (E10) Mouse mAb pERK2 Catalog # 9106S **Anti P-ERK1/2** (1:2000)	Cell signaling Technology, Inc.Danvers, MA U.S.A.		
Hybridom Anti-Myc antibody **Anti myc** (1:200)	**ATCC® Number:**CRL-1729 ™		
PRAK (A-7) Mouse monoclonal IgG_1 Catalog # sc-46667 **Anti MK5 A7** (1:500)	Santa Cruz Biotechnology, Inc. Santa Cruz, CA, U.S.A.		
Anti-MAPK6 (612-721) mAb 0,05 mg, 0,45 mg/ml Catalog # H00005597-M02 **Anti ERK3** (1:500)	Abnova, Neihu District, Taipei City, Taiwan		

4 METHODS

4.1 Construction of expression vectors

4.1.1 MidiPrep

QIAGEN® Plasmid *Plus* Midi Kit was used according to protocols from the manufacturer for the purification of plasmids. The concentrations were measured in ng/µl by using the software NanoDrop 1000 V3.8 and the instrument NanoDrop® ND-1000 spectrophotometer (Thermo Fisher Scientific, Wilmington, U.S.A.).

4.2 Mammalian cell culture techniques

4.2.1 Cell culture

The H1299 cells were cultured in DMEM supplemented with 10 % FBS and 1 % antibiotics (10000 U/ml penicillin and 10 mg/ml streptomycin). The cell cultures were grown in Thermo-scientific nunc® Easy Flasks™, and incubated in HERAcell® 150i CO_2 incubator with following conditions: 37 °C, 5 % CO_2 and 80-95 % relative humidity.

4.2.2 Harvesting cells and cell splitting

The PBS media (stored at room temperature) and Trypsin (stored at – 20 °C, once opened: 2-4 °C) was pre-warmed to 37 °C. Media covering the monolayer of cells in the T-flask was discarded. In order to have optimal effect of Trypsin, the bottom of the T-flask was washed quickly with 0.2 ml PBS/cm^2 surface. To dethatch the cells from the surface, 40 µl Trypsin/cm^2 was added and the flask rocked gently to make sure that the entire monolayer was covered. The T-flask was incubated at 37 °C for 2-5 minutes and checked under microscope to confirm that all the cells were floating and if there were any lumps of cells. Appropriate amount of medium was added to dilute and neutralize Trypsin. When the cells were not counted and seeded for transfection, they were split 2-4 times a week according to confluence and planned assays.

4.2.3 Counting cells

A Bürker Counting Chamber was used for counting of the cells. The chamber was cleaned with water and ethanol, and the coverslip was moisturized by water in order to fix it on the counting chamber. The cell suspension was mixed gently by pipetting up and down 8 times to ensure that cell lumps was dispersed to form a homogenous cell suspension. 500 µl cell suspension was pipetted to an Eppendorf tube. From this, 20 µl was pipetted to the counting chamber under the cover slip to be drawn into place by capillary forces. The counting chamber was placed under the microscope, and as many A windows in the chamber needed to reach 200 cells was counted. The viable cell concentration per ml was calculated using the following formula:

$$\frac{Number\ of\ cells\ x\ 10\ 000}{Number\ of\ A\ windows} = cell\ number\ per\ ml\ suspension$$

4.2.4 Seeding cells

The amount of cell suspension needed per well was calculated:

$$\frac{Cells\ per\ well\ x\ number\ of\ wells}{Cell\ number\ per\ ml\ suspension} = ml\ cell\ suspension$$

The calculated volume of cell suspension was pipetted to a centrifuge tube and growth medium was added to form a master suspension. The amount growth medium added was calculated according to number and type of wells used: media used for a 6 well plate was calculated from the total volume of 2 ml per well of cell suspension and media, and the total volume for a 60 mm well was 3 ml. The master suspension was plated into the wells and placed in the incubator overnight.

4.2.5 Transfection with Lipofectamine® 2000

Cells seeded 24 hours before (or when the confluence was 70-80 %) were used for transfection. A master mix of Lipofectamine® 2000 and Opti-MEM® was prepared (3 µl Lipofectamine® 2000 and 247 µl Opti-MEM® per sample) and incubated at room temperature for at least 5 minutes. 250 µl Opti-MEM® was pipetted in each autoclaved Eppendorf tubes (one tube per sample). Depending on the planned assay, appropriate amount of plasmid was pipetted into the tubes. 250 µl master mix was added to the tubes and incubated for 20 minutes at room temperature. In the meantime, the media from the wells was discarded and 500 µl Opti-MEM® was added to each well before incubating at 37 °C again. After 20 minutes, all the contents in each Eppendorf tube were pipetted to the wells and then

incubated at 37 °C. After 4-6 hours, 4 ml growth medium was pipetted to each well when using 60 mm wells or 2 ml when using a 6 plate well.

4.2.6 Harvesting cells after transfection (cell lysis)

Growth medium was removed 24-48 hours post transfection, and a washing step with 2 ml PBS was carried out twice. After discarding PBS, 300 µl of lysis buffer (with phosphatase and protease inhibitors) appropriate for the planned assay was distributed evenly in each well. After 1 min, the cells were collected using a rubber cell scraper and the cell lysates was transferred to autoclaved Eppendorf tubes. The lysates were sonicated briefly (for 2 seconds) and incubated on ice for 20 minutes. After centrifuging the lysates at 13 000 rpm for 15 min. at 4 °C, the supernatant was carefully pipetted to autoclaved Eppendorf tubes while ensuring not to transfer debris to the new tubes. The cell lysates were stored at -70 °C when not used the same day.

4.3 Immunoprecipitation

Cell lysates stored at -70°C were thawed on ice. Magnetic beads (10 µl per sample; 5 µl when using magnetic beads pre-coated with antibodies) were washed 3 times with 500 µl ice-cold lysis buffer with phosphatase inhibitor (type of lysis buffer used varied according to planned assays). The beads were re-suspended in ice-cold lysis buffer with phosphatase and protease inhibitors. When using magnetic beads without antibodies, the cell lysates were added 10 µl antibodies and incubated on a rotator wheel at 4 °C for 60 min. This step was skipped when magnetic beads pre-coated with antibodies were used. 10 µl washed magnetic beads (5 µl when pre-coated with antibodies) were added to each sample and incubated on a rotator wheel at 4 °C for 1 hour (3 hours when pre-coated). The mix of lysate and magnetic beads was washed first 3 times with 500 µl ice-cold lysis buffer with phosphatase inhibitor, and then 2 times with 500 µl 50 mM Tris [pH 7.5]. Proteins were eluted with 40 µl sample reducing buffer (1.4 x) per sample and incubated at 70 °C for 10 min. The samples were cooled and stored at -70 °C when not used for SDS-PAGE and WB the same day.

4.4 Western blot

4.4.1 SDS-PAGE

39 µl cell lysate was added 15 µl LDS Sample Buffer (4x) and 6 µl Sample Reducing Agent (10x). The samples were incubated at 70 °C for 10 min. 40 ml NuPAGE® MES SDS Running Buffer (20x) was diluted with 800 ml dH_2O. The manufacturer's protocol was followed to prepare further for sample loading. 15-20 µl of each sample and 5 µl SeeBlue® Plus2 Pre-Stained Standard was loaded into the wells of the SDS-PAGE gel. When Magic Marker® was used, it was loaded 1 µl of it. The electrophoresis was run at 200 V for 45 minutes when analyzing CID-fragments of SRC-3, and for 1 hour and 30 minutes when analyzing full-length SRC-3.

4.4.2 Blotting

Prior to blotting a nitrocellulose membrane was washed for a minimum of 5 minutes in blotting buffer, and 4 filter papers and 5-6 blotting pads were soaked in blotting buffer. A blotting unit was prepared by layering these components to a sandwich as illustrated in the figure below:

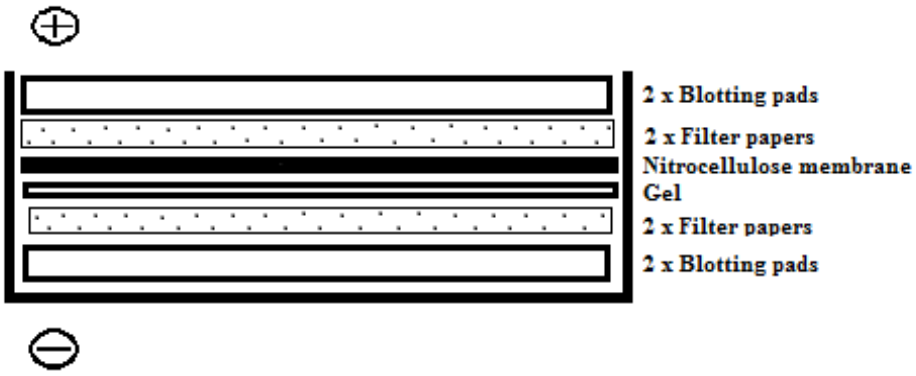

Figure 5: Illustration of the blotting unit.

The blotting unit was placed in an XCell Sure Lock™ Mini-cell. The inner chamber was filled with blotting buffer, and the outer chamber was filled with fresh, cold deionized water. The blot was performed by the NuPage blot program at 30 V (160 mA) for 2 hours for full-length SRC-3 (1 hour 30 minutes for CID-SRC-3). After the blotting, the membrane was washed for 1 hour with 25 ml blocking buffer on a Gyro-Rocker. The membrane was then transferred to a 50 ml centrifuge tube containing 5 ml blocking buffer, 5 µl Tween 20 and primary antibodies in dilutions as described in section 3. The tube was incubated overnight on

a rotator at slow speed at 4 °C. Next day, the membrane was washed 3 x 5 minutes with washing buffer by placing the beaker on the Gyro-Rocker. The secondary antibody was diluted (1:10 000) in 5 ml washing buffer in a 50 ml centrifuge tube covered with aluminum foil in order to protect the antibodies against light. The membrane was transferred to this tube and incubated on a rotator at slow speed for 1 hour at room temperature. The membrane was washed 2 x 5 minutes with washing buffer. The protein bands were detected by using the ODYSSEY® Sa Infrared Imaging System.

4.5 *In vitro* kinase assay

The kinase solutions were prepared by mixing kinase buffer, GST-SRC-3CID, Milli-Q water and appropriate amount of kinase analyzed (Appendix 1) Eppendorf tubes containing the kinase assay mix were incubated at 30 °C for specific time intervals (Appendix 1). The kinase reaction was stopped by adding LDS Sample Buffer and Sample Reducing Agent, and then incubated at 70 °C for 10 minutes prior to WB analysis. To confirm phosphorylation of S857 at CID WT, anti P-S857 SRC-3 antibody (1:2000) was used.

5 RESULTS

In contrast to the results published by Long et al do results from our group, using a radioactive *in vitro* kinase assay, indicate that ERK3 does not phosphorylate SRC-3 very efficiently (Tømte, Almahi and Seternes, unpublished results). Closer inspection of the sequences around the Serine 857 of the SRC-3 (RAV**S**L) reveals that this serine is not within an optimal sequence for phosphorylation by MAP kinases (S/T-P). The sequence around S857 of SRC-3 resembles more an optimal motif for phosphorylation by protein kinase A (PKA) or MAPKAP kinases (R-X-X-S/T). This site can be phosphorylated by PKA and IKK *in vitro* (44). As we know that MAPKAPK5 is a direct downstream effector of ERK3, we could observe that MK5, rather than ERK3, could phosphorylate SRC-3 *in vitro*. In order to investigate if this was true also *in vivo*, we needed to generate a phospho-specific antibody against this site. A phosphospecific antisera against S857 of SRC-3 was developed in collaboration with the Division of Signal transduction therapy (DSTT) at the University of Dundee. In order to use this antibody on western blots using cell extract, we had to verify that the antibody could recognize SRC-3 phosphorylated on S857. In addition, we needed to optimize the western blot protocol.

5.1 Optimizing and validating anti-phospho-SRC-3 antibody

5.1.1 Dilutions of anti-phospho-SRC-3 antibody

The antibody anti P-S857 SRC-3 (2nd bleed, sheep) is designed to specifically recognize phosphorylated S857 at the SRC-3 protein or its fragments. This assay was performed to confirm that the antibody recognized SRC-3 phosphorylated on S857 and to find the optimal concentration of this antibody when used as a primary antibody for WB analysis. We tested the dilutions 1:500, 1:1000 and 1:2000. Glutathione S-transferase (GST) served as a control while testing the GST-SRC-3 fragment fusion proteins of wildtype: GST-SRC-3CID WT (hereafter CID WT), and a mutant of the CID domain where the phospho-acceptor site Serine 857 is changed to an unphosphorylatable alanine: GST-SRC-3CID S857A (hereafter CID S857A), with and without MK5. In Figure 6, we can see that CID WT incubated with MK5 is phosphorylated to a significantly greater extent compared to CID WT alone or CID S857A incubated with MK5. The blot with anti P-S857 SRC-3 dilution 1:2000 (Figure 6C) shows greater specificity towards S857 phosphorylation and gives clearer bands. This dilution will be used for further western blot analysis.

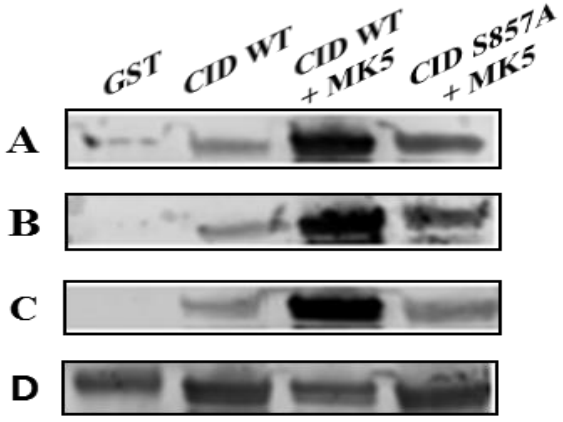

Figure 6: Optimizing anti P-S847 SRC-3 antibody for use as a primary antibody for WB analysis. WB analysis of cell extracts of cell transfections with GST, CID WT, CID WT co-transfected with MK5 and CID S857A co-transfected with MK5. Anti P-S857 SRC-3 antibody used as primary antibody with various dilutions; 1:500 (A), 1:1000 (B) and 1:2000 (C). The membrane C was incubated a second time with GST-antibody 1:200 (D).

A second incubation of this membrane with GST-antibody was conducted in order to confirm equal loading to each lane (Figure 6D). The minor differences in band intensity do not explain the differences seen in the phosphorylation of S857. In other words, the results from co-incubation of CID WT and MK5 are not a consequence of extensive loading of cell extract in this lane.

5.1.2 Dilutions of CID WT co-incubated with MK5 analyzed with anti P-S857 SRC-3 antibody

We wanted to test if the detection of the phosphorylated SRC-3 was linear using different dilutions of phosphorylated GST-SRC-3 and anti-phospho-SRC-3 as primary antibody. Concentrations 1:1000 (Figure 7 A) and 1:2000 (Figure 7B/C) of the antibody were tested. This experiment confirmed our results from the previous test of the anti-phospho-SRC-3 antibody that showed the 1:2000 dilutions to be more specific and give clearer bands compared to 1:1000 dilutions. We can see in Figure 7 that the phosphorylation of S857 at CID WT by MK5 is increasing with increasing concentrations (from right lanes to left side). This verifies the anti-phospho-SRC-3 antibody to be very specific. Quantitative analysis of band intensity implies the phosphorylation of S857 at CID WT by MK5 to be linear, but more parallels are needed to statistically confirm this correlation. To control for amount of GST-SRC-3 loaded to each well, the second membrane (1:2000 anti P-S857 SRC-3) was incubated with GST-antibody (Figure 7C). As wished, the band intensities are decreasing with increasing dilutions.

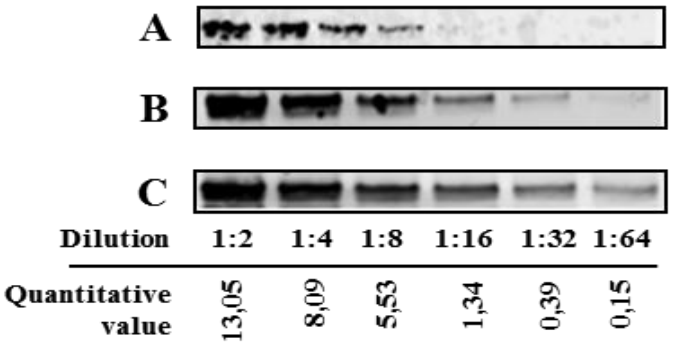

Figure 7: Analysis of different dilutions of CID WT co-expressed with MK5 using anti P-S857 SRC-3 as primary antibody. Cell extract of CID WT and MK5 was diluted with 2 x LDS buffer. The dilutions and quantitative values are specified at the bottom of each lane. The anti P-S857 SRC-3 antibody was diluted 1:1000 (A) and 1:2000 (B). Membrane in B was further incubated with GST-antibody1:200 (C).

5.2 *In vitro* kinase assays with SRC-3 CID as substrate

Same conditions were kept for the *in vitro* kinase assays in order to be able to compare the results. It was investigated whether the distinct kinases were upstream of SRC-3 CID and had SRC-3 CID as their substrate. The kinases we studied were MK5, MK2, ERK2, ERK3 and p38.

5.2.1 *In vitro* kinase assay with CID and MK5

WB analysis of concentrations of 5, 10, 20 and 40 ng MK5 was assessed after the kinase reaction had been incubated for 15 minutes (left panel Figure 8), and 100 ng MK5 reaction proceeded for 5, 10, 15 and 30 minutes (right panel Figure 8). Figure 8 shows protein bands of membranes incubated with anti P-S857 SRC-3 antibody (A) and GST-antibody (B). The band intensity for row A left panel is increasing proportionally (Appendix 2), which indicates linear phosphorylation of CID by MK5. The phosphorylation is not linear for 100 ng MK5 at different time intervals as seen in row A right panel (Appendix 3). This can be explained by the phosphorylation process happening too fast at concentration of 100 ng MK5, and the process is outside linearity already before 5 min. The purpose of incubation with GST-antibody is to check for equal loading, as described earlier, and in this assay we want to analyze the amount of CID in the lanes in the right and left panel. Corresponding amounts of CID was added to the kinase reactions in the left panel, and the amount of CID is the same in all lanes of the right panel since 20 µl solutions were taken out at different time intervals from the same kinase reaction. This is reflected by the results seen in row B in the right panel, and to some extent in the left panel.

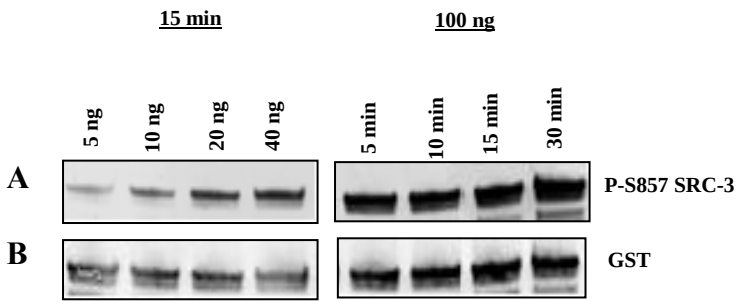

Figure 8: WB analysis of *in vitro* kinase assay with CID and MK5. Left panel: Kinase reaction containing 5, 10, 20 and 40 ng MK5 and CID incubated for 15 min. **Right panel:** Kinase reaction containing 100 ng MK5 and CID incubated for 5, 10, 15 and 30 min. Membrane incubated with anti P-S857-SRC-3 antibody 1:2000 (A) and GST-antibody 1:200 (B).

5.2.2 *In vitro* kinase assay with CID and MK2

This kinase assay was conducted with the same conditions as the previous kinase assay. The MK2 solution had a 60 fold higher concentration calculated in U/mg compared to MK5, and was therefore diluted by a factor of 60 in order to compare the results with MK5. To facilitate comparison of MK2 and MK5, the results for MK2 are shown in the same concentration labels (ng/µl) as MK5 since the concentration is corresponding in U/mg. The left panel results for MK2 (Figure 9) corresponds to left panel results of MK5 (Figure 8, Appendix 4), but in Figure 9 right panel we can see different outcome even though same amounts of kinases and CID were mixed for the kinase reactions. One explanation for these results is the possibility of CID degradation before adding it to the reaction. The Eppendorf tube with CID had been thawed on ice and then frozen before thawed a second time when used for the 100 ng MK2 reaction. This is reflected in Figure 9 row B as the amount of CID added to 100 ng MK2 reactions are same in each lane (right panel) and all the bands have much lower intensity compared to left panel (CID from distinct Eppendorf tubes). Low amounts of CID gives less phosphorylation (row A, right panel) despite high concentration (100 ng) of MK2, which explains why phosphorylation of CID by MK2 is not outside linearity (Appendix 5).

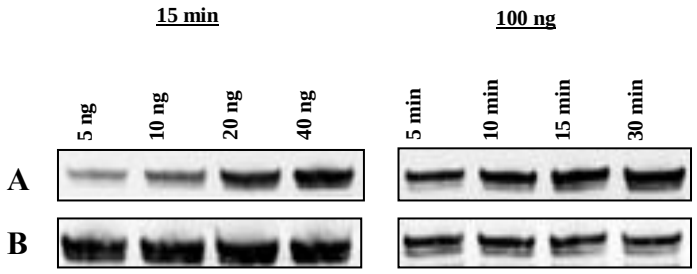

Figure 9: WB analysis of *in vitro* kinase assay with CID and MK2. Left panel: Kinase reaction containing CID and 5, 10, 20 and 40 ng MK2 respectively, incubated for 15 min. **Right panel:** Kinase reaction containing CID and 100 ng MK2 incubated for 5, 10, 15 and 30 min. Membrane incubated with anti P-S857 SRC-3 antibody 1:2000 (A) and GST-antibody 1:200 (B).

5.2.3 *In vitro* kinase assay with CID and ERK2 and ERK3

ERK3 phosphorylates CID-SRC-3 at S857 to greater extent than ERK2 (Figure 10). The phosphorylation is not proportionally increasing.

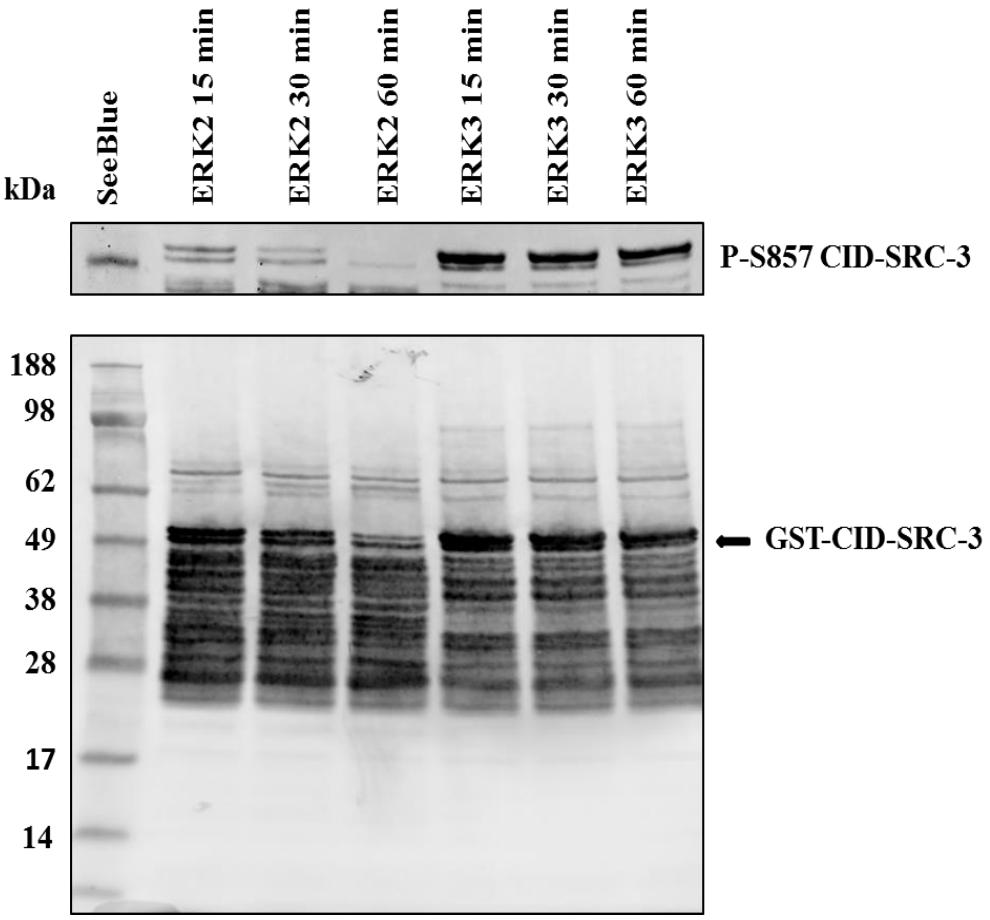

Figure 10: WB analysis of *in vitro* kinase assay with CID + ERK2 and CID + ERK3. Upper panel: Kinase reaction containing ERK2 equivalent to 100 ng MK5 and CID incubated for 15, 30 and 60 min (left), and likewise kinase reaction of ERK3 (right) is represented. Primary antibody: Anti P-S857 SRC-3 (1:2000). **Lower panel:** Blot in upper panel was further incubated with GST-antibody (1:200).The arrow indicates GST-CID-SRC-3 phosphorylation. SeeBlue® was used for band identification.

5.2.4 *In vitro* kinase assay with CID and ERK3 or p38

Compared to ERK3, p38 does not phosphorylate CID SRC-3 at S857 efficiently, but the phosphorylation is increasing with time.

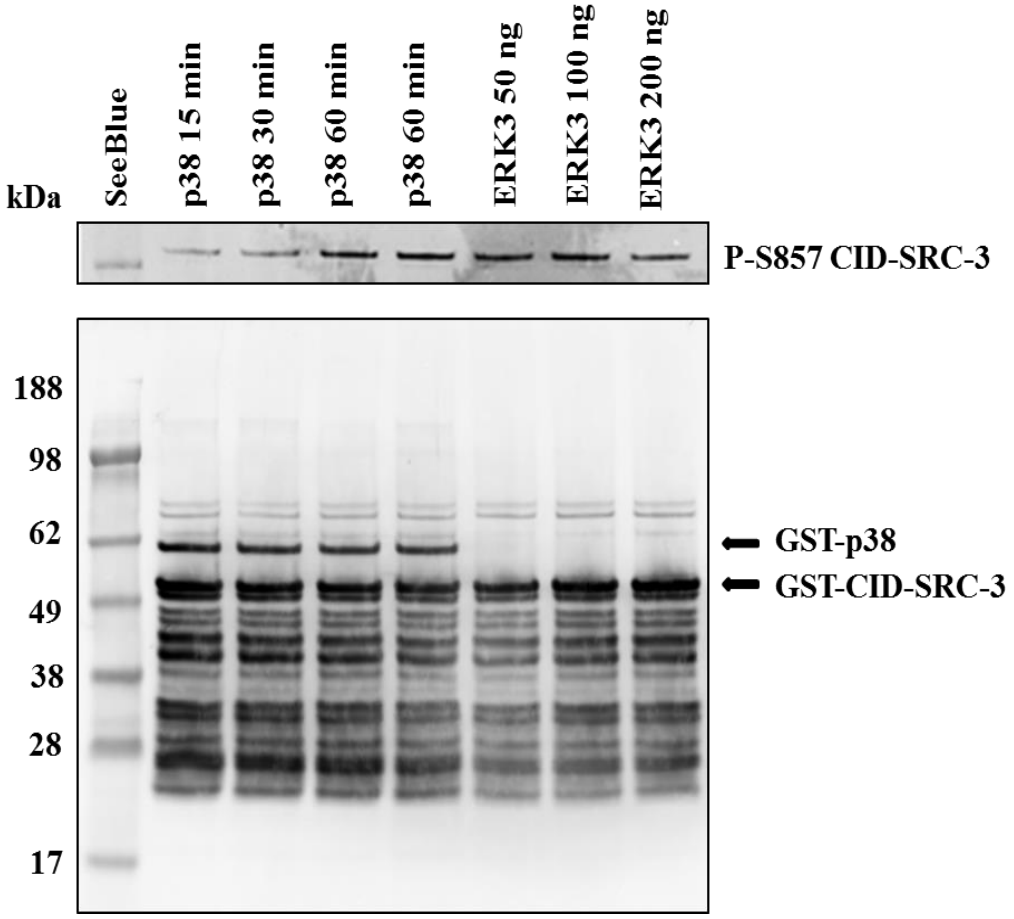

Figure 11: WB analysis of *in vitro* kinase assay with CID + p38 and CID + ERK3. Upper panel: Kinase reaction containing p38 equivalent to 100 ng MK5 and CID incubated for 15, 30 and 60 min (left) and 50, 100, 200 and 300 ng ERK3 incubated with CID for 15 min. Primary antibody: Anti P-S857 SRC-3 (1:2000). **Lower panel:** Blot in upper panel was further incubated with GST-antibody (1:200). The arrows indicate GST-p38 and GST-CID-SRC-3 phosphorylation. SeeBlue® was used for band identification.

5.2.5 *In vitro* kinase assay – comparison of MK2, MK5, ERK2, ERK3 and p38

In Figure 12 we can see that equal amounts of MK2 and MK5 phosphorylate S857 at CID-SRC-3 to a significantly greater extent compared to ERK2, ERK3 and p38, which has similar effect on S857 phosphorylation.

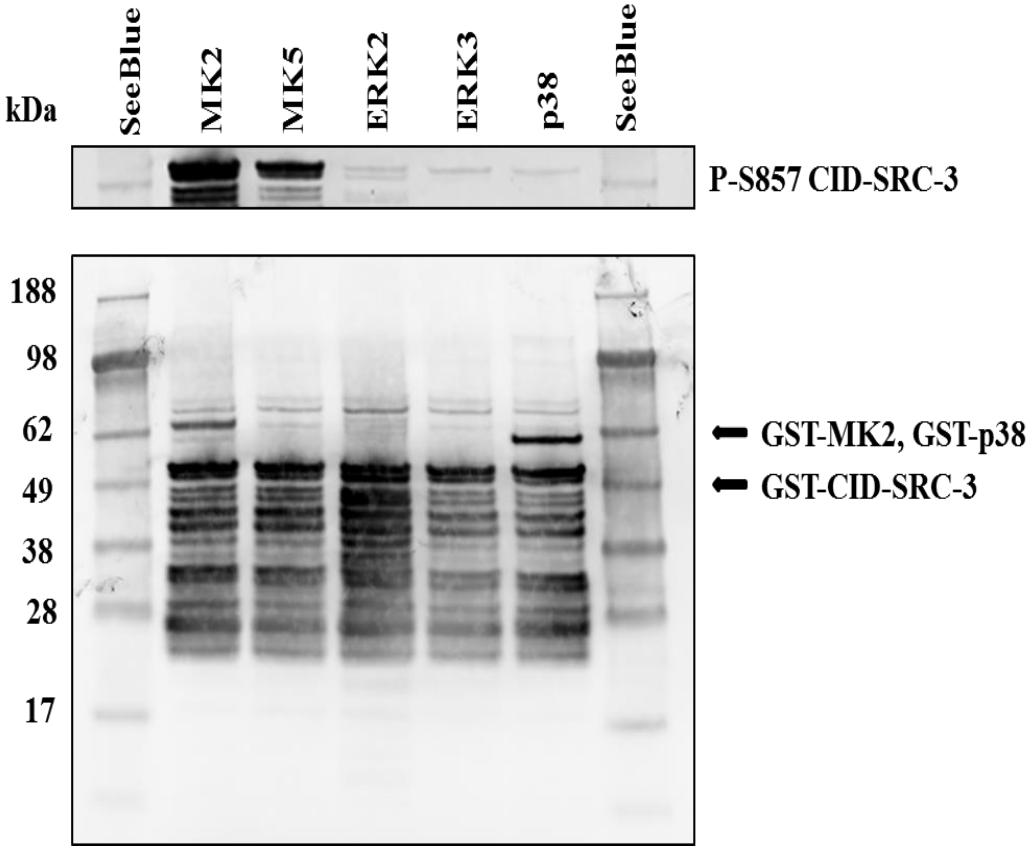

Figure 12: WB analysis of *in vitro* kinase assay with CID + MK2, MK5, ERK2, ERK3 and p38. Upper panel: Kinase reaction containing CID and MK2, MK5, ERK2, ERK3 and p38 of equal amounts (equal to the kinase activity of 100 ng MK5) incubated for 15 min. Primary antibody: Anti P-S857 SRC-3 (1:2000). **Lower panel:** Blot in upper panel was further incubated with GST-antibody (1:200). The arrows indicate GST-MK2, GST-p38 and GST-CID-SRC-3 phosphorylation. SeeBlue® was used for band identification.

5.3 Immunoprecipitation method for full length SRC-3

The IP method, followed by WB analysis, was optimized by altering parameters such as type of lysis buffer, sonication versus vortex mixing (cell lysis step), and type of magnetic beads and antibodies, in addition to their incubation-time (data not shown). The most efficacious method tested for IP, from transfection to WB analysis, and materials used are described below.

- Transfection method: Lipofectamine® 2000. The cells were harvested after 24 hours.
- Method for harvesting cells after transfection (with sonication for 2 seconds); see section 4.2.6. Lysis buffer: HA –lysis buffer with phosphatase and protease inhibitors.
- 5 µl of Anti-FLAG® M2 Magnetic Beads washed with HA-lysis buffer with phosphatase inhibitors was added to each lysate and incubated at 4 °C for 3 hours. The IP method described in section 4.3 was followed.
- SDS-PAGE was conducted as described in section 4.4.1. 20 µl of each lysate was used and the analysis was run for 45 minutes at 200 V and 120 mA.
- The WB program was run for 2 hours at 30 V and 160 mA.

The results are presented in Figure 13 for analysis of both IP lysates and whole cell extracts (WCEs), and shows that Myc-ERK3 does not increase the levels of Flag-SRC-3 phosphorylation.

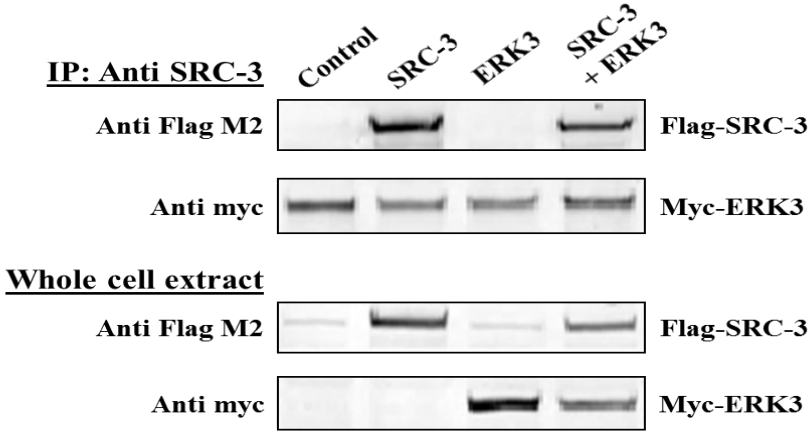

Figure 13: Myc-ERK3 does not increase levels of Flag-SRC-3 phosphorylation. 500 000 H1299 cells per 60 mm wells were transfected with either 1000 ng Flag-SRC-3, 1000 ng Myc-ERK3 or 1000 ng of both plasmids. Non-transfected cells serve as control. Cells were lysed with HA-lysis buffer and Flag-SRC-3 was immunoprecipitated (incubation with 5 µl Anti-FLAG® M2 Magnetic Beads for 3 h). IP lysates and WCEs were analyzed by SDS-PAGE and WB. Anti P-S857 SRC-3 (1:2000) was used to determine the levels of SRC-3 phosphorylated at S857, and anti myc for the detection of ERK3 levels. The assay was repeated and the results are representative for both parallels.

5.4 *In vivo* kinase inhibitor assays with endogenous SRC-3

It was investigated whether distinct kinases could be upstream of endogenous SRC-3 *in vivo* by using WB analysis of IP lysates and WCEs of various transfected kinases inhibitors.

5.4.1 *In vivo* kinase assay with MEK-inhibitor and p38-inhibitor

This assay with H1299 cells treated with MEK-inhibitor and p38 inhibitor was carried out to test if inhibition of endogenous MEK or p38 altered the phosphorylation of the S857 residue of endogenous SRC-3. The results are shown in Figure 14 where we can see more than 85 % decrease of SRC-3 phosphorylation (Appendix 6) when p38 is inhibited. In comparison, MEK-inhibition does not decrease the phosphorylation of SRC-3 (the phosphorylation is in fact increased by 76 % by MEK-inhibition). The phosphorylation of ERK2, which is downstream of MEK, is significantly reduced as expected. However, the effect of p38-inhibition on ERK2 phosphorylation was not expected.

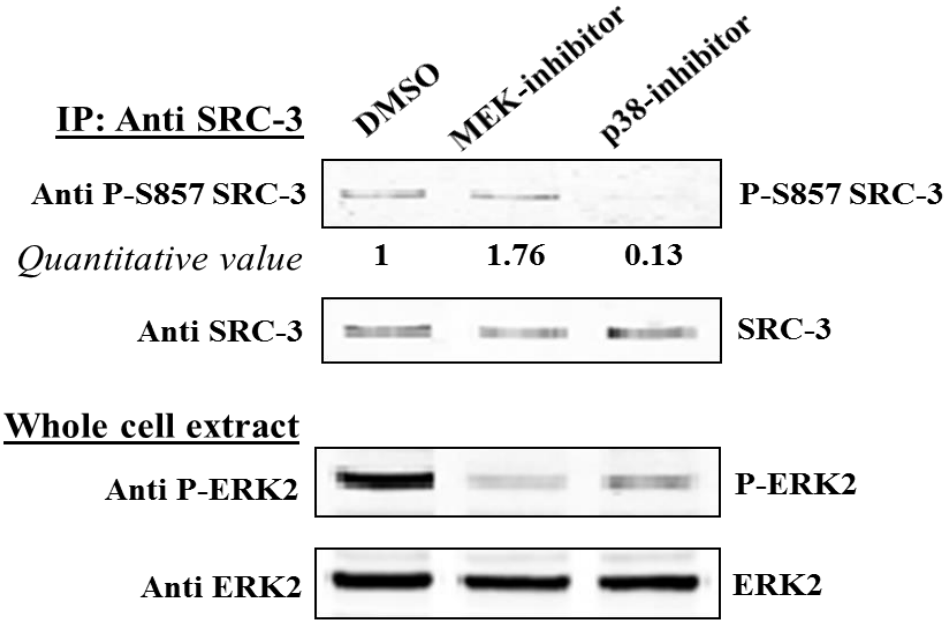

Figure 14: The p38-inhibitor decrease the levels of endogenous SRC-3 phosphorylated at S857 *in vivo*. 500 000 H1299 cells per 60 mm wells were stimulated for 2 h with 10 µM of either DMSO (control), MEK-inhibitor or p38-inhibitor. Cells were lysed with MKK lysis buffer and endogenous SRC-3 was immunoprecipitated (PureProteome™ Protein G Magnetic Beads incubated with 20 µl SRC-3 antibody for 1 h). IP lysates and WCEs were analyzed by SDS-PAGE and WB. Anti P-S857 SRC-3 (1:1000) was used to determine the levels of endogenous SRC-3 phosphorylated at S857. Staining with anti P-ERK2 (1:2000) and anti ERK2 (1:1000) confirm successful inhibition of MEK and p38. Quantitative values are specified at the bottom of each lane of P-S857 SRC-3. The assay was repeated and the results are representative for both parallels.

5.4.2 *In vivo* assay with Anisomycin

This assay was carried out to investigate how an increase of p38 by stimulation with anisomycin would affect the phosphorylation of endogenous SRC-3 at S857. The results are presented in Figure 15, which shows a raise in levels of phosphorylated S857 SRC-3 as well as levels of phosphorylated p38 compared to the control.

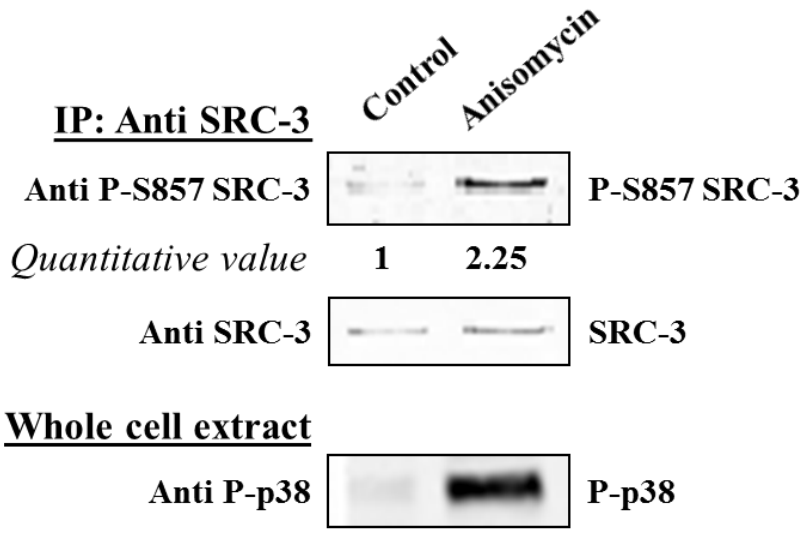

Figure 15: Anisomycin-induced increase in p38 increases the phosphorylation of SRC-3 at S-857 *in vivo*. 500 000 H1299 cells per 60 mm wells were stimulated for 30 min with 25 µg/ml Anisomycin. Untreated cells serve as control. Cells were lysed with MKK lysis buffer and endogenous SRC-3 was immunoprecipitated (PureProteome™ Protein G Magnetic Beads incubated with 20 µl SRC-3 antibody for 1 h). IP lysates and WCEs were analyzed by SDS-PAGE and WB. Anti P-S857 SRC-3 (1:1000) was used to determine the levels of endogenous SRC-3 phosphorylated at S857. Staining with anti SRC-3 (1:2000) was used to determine the levels of total SRC-3, and anti P-p38 (1:1000) to check the levels of p38. Quantitative values are specified at the bottom of each lane of P-S857 SRC-3. The assay was repeated and the results are representative for both parallels.

5.4.3 *In vivo* assay with the PKA-inhibitor H-89

Figure 16 shows the results of an *in vivo* assay with the PKA-inhibitor H-89. Inhibition of PKA does not alter the level of endogenous SRC-3 phosphorylation at S857.

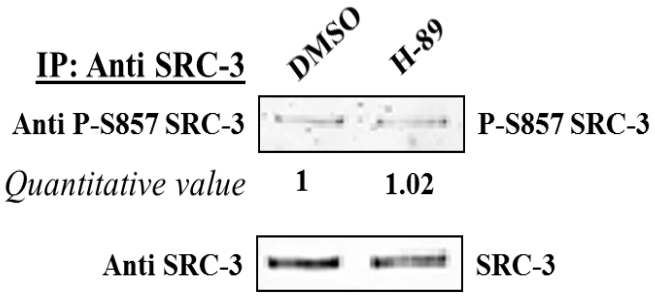

Figure 16: The PKA-inhibitor H-89 does not affect the levels of endogenous SRC-3 phosphorylated at S857 *in vivo*. 500 000 H1299 cells per 60 mm wells were stimulated for 2 h with 10 µM of the PKA-inhibitor H-89. Cells were lysed with MKK lysis buffer and endogenous SRC-3 was immunoprecipitated (PureProteome™ Protein G Magnetic Beads incubated with 20 µl SRC-3 antibody for 1 h). IP lysates were analyzed by SDS-PAGE and WB. Anti P-S857 SRC-3 (1:1000) was used to determine the levels of endogenous SRC-3 phosphorylated at S857. Staining with anti SRC-3 (1:1000) shows total amount of SRC-3. Quantitative values are specified at the bottom of each lane for P-S857 SRC-3.

5.5 siRNA knockdown of MK5 and ERK3

siRNA mediated knockdown of MK5 and ERK3 was assessed, and the results shows minimal effect on the phosphorylation of SRC-3 (at least there is no decrease of phosphorylation) as shown in Figure 17.

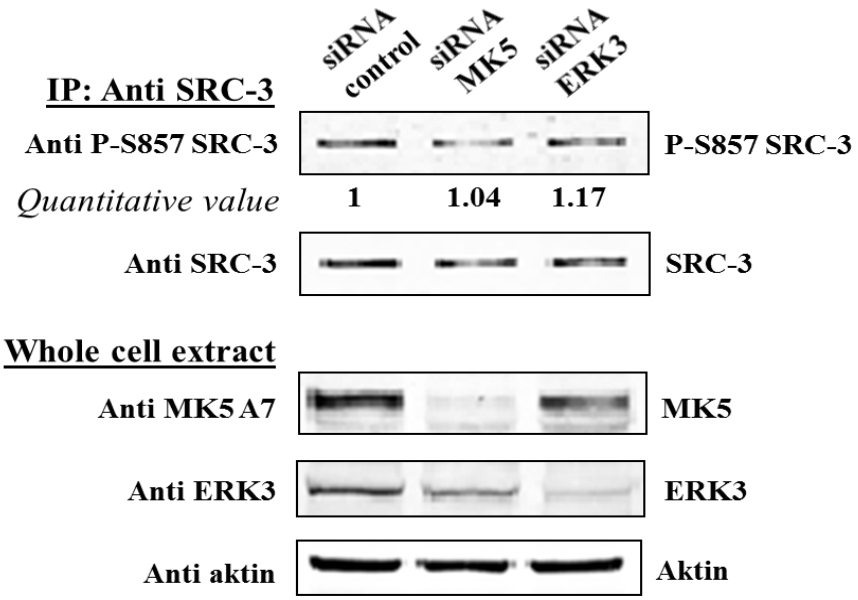

Figure 17: siRNA mediated knockdown of ERK3 does not affect phosphorylation of endogenous SRC-3 at S857. 500 000 H1299 cells per 60 mm wells were transfected with 20 nM of either control (scrambled) siRNA, siRNA MK5 or siRNA ERK3. Cells were lysed with MKK lysis buffer after 48 h and endogenous SRC-3 was immunoprecipitated (PureProteome™ Protein G Magnetic Beads incubated with 20 µl SRC-3 antibody for 1 h). IP lysates and WCEs were analyzed by SDS-PAGE and WB. Anti P-S857 SRC-3 (1:1000) was used to determine the levels of endogenous SRC-3 phosphorylated at S857. Staining with Anti MK5 A7 (1:500) and anti ERK3 (1:500) confirms knockdown of MK5 and ERK3, respectively. Staining with anti-aktin (1:1000) was used as control for loading. Quantitative values are specified at the bottom of each lane of P-S857 SRC-3. The assay was repeated and the results are representative for both parallels.

6 DISCUSSION

SRC-3 plays an important role in various cellular processes and is implicated in inflammation, angiogenesis, proliferation, chemo resistance, tumor growth, invasion and metastasis. This oncogenic nuclear receptor coactivator is reported to be overexpressed in multiple human cancers, e.g. breast, lung and prostate cancer. SRC-3 is a coactivator for nuclear hormone receptors and numerous transcription factors. This property enables it to control multiple growth pathways simultaneously, and it holds future promise for clinical cancer therapy (38, 45, 46).

Several research groups are studying SRC-3 worldwide; some are focusing on elucidating up- and downstream targets of SRC-3, while others are studying possible inhibitors. The SRCs are large proteins which previously were not considered to be "druggable" targets. However, the great efforts have paid off as a result of the recent discovery of two small-molecule inhibitors (SMIs) of SRC-1 and SRC-3; Gossypol and Bufalin (47, 48). If Bufalin, or future, SMIs of SRCs succeed to enter clinical trials, and hopefully manage to reach the clinic as anti-cancer therapeutics, it will be beneficial for various groups of cancer patients. Gossypol (also called Ascenta Therapeutics -101) is currently in clinical trials for the treatment of prostate and lung cancer, and leukemia. It is noteworthy that better understanding of up- and downstream targets of SRCs will be advantageous in optimizing cancer therapy when considering the possibility to inhibit protein kinases, phosphatases or other signaling molecules, which could potentially be up regulated as a consequence of SRC inhibition, with combinatorial therapeutics.

Long et al (43) have reported that ERK3 phosphorylate SRC-3 at the S857 residue, but our findings do not support the theory that ERK3 is an upstream regulator of SRC-3 phosphorylation at S857. The results of our *in vitro* and *in vivo* assays indicate the p38 MAPK pathway, rather than the ERK3 pathway, to be involved in the phosphorylation of SRC-3 at S857.

Optimizing and validating anti-phospho-SRC-3 antibody

A highly specific antibody for the SRC-3 phosphorylation of S857 was a prerequisite for this study in order to obtain reliable results. The optimized dilution of the custom-made antibody anti-P3857 SRC-3 was determined to be 1:2000. The antibody was validated and ascertained to be very specific as it did not bind to the mutant of the CID (CID S857A). Additional analysis of various dilutions of CID WT co-incubated with MK5 (section 5.1.2) further strengthened our presumptions of this antibody's specificity and the notion of 1:2000 dilution being the optimized dilution. Dilutions of 1:1000 were used when analyzing IP lysates due to low amounts of endogenous SRC-3 in the cells.

MK5 phosphorylates SRC-3 at S857 *in vitro*, but not *in vivo*

The results of the *in vitro* assay of MK5 demonstrates linear phosphorylation at concentrations between 5-40 ng for kinase reactions incubated for 15 minutes, but not for 100 ng MK5 reactions incubated for 5-30 minutes. siRNA mediated knockdown of MK5 resulted in no change in the levels of phosphorylated S857 residues of endogenous SRC-3 *in vivo* when compared to the control (Appendix 6). Thus, MK5 does not appear to be a direct upstream kinase for SRC-3 in living cells.

ERK3 phosphorylates SRC-3 at S857 *in vitro*, but not *in vivo*

In vitro assays show that ERK3 phosphorylates the S857 residue of SRC-3 more efficiently than ERK2. We also repeated the immunoprecipitation assay described in the study of Long et al by first optimizing an IP method for full length SRC-3, and then analyzing IP of Flag-SRC-3 co-transfected with Myc-ERK3. Myc-ERK3 was found to not increase the levels of Flag-SRC-3 phosphorylation at S857 *in vivo*. The observations of siRNA mediated knockdown analysis of ERK3 *in vivo* are also consistent with these findings. The *in vivo* assays were repeated with corresponding results. Based on our results so far, we wanted to investigate other MAPKs or MAKPAKPs to be upstream kinases of SRC-3.

ERK2 phosphorylates SRC-3 at S857 *in vitro*

Our data from *in vitro* assays indicated that ERK2, like ERK3 and p38, phosphorylates SRC-3 at S857 with little efficiency. By using MEK-inhibitor (which inhibits the basal activity of the MAPKAP kinases MSKs, MNKs and RSKs), we also demonstrate that ERK1/2 cannot be the upstream kinases of SRC-3 *in vivo*. Based on these results, we find the MAPKAPKs RSKs and MNK2 (which are downstream targets of ERK1/2) not to be directly involved in SRC-3 phosphorylation at S857. We also tested the *in vivo* effect of PKA on the phosphorylation of S857 by using the PKA-inhibitor H-89. Compared to the control, the results show no effect on the phosphorylation of endogenous SRC-3 at S857. H-89 inhibits MSK1 with equal potency as PKA, and inhibits the RSKs as well (49). This suggests that the MAPKAP kinases RSKs and MSK1 are not involved in the SRC-3 phosphorylation at S857. Wu et al have reported PKA to phosphorylate S857 of SRC-3 in HEK293 cells in contrast to our study, which were carried out by using H1299 lung cancer cells. The H1299 cells have K-Ras mutations and are p53 null, which could interfere with normal cross-talk between the different signaling pathways. This might explain the interesting effect seen on ERK2 phosphorylation, which notably decreases upon p38-inhibition.

p38 does not phosphorylate SRC-3 at S857 *in* vitro, but is involved *in vivo*

In vitro assays of p38 did not show direct phosphorylation of SRC-3 S857. Conversely, MK2 demonstrated linear phosphorylation at concentrations between 5-40 ng for kinase reactions incubated for 15 minutes, and also for 100 ng MK5 reactions incubated for 5-30 minutes *in vitro*. MK2 is a direct downstream target of the p38 pathway, and based on our data, we wanted to investigate if this pathway could be upstream of SRC-3 *in vivo*.

The results from our *in vivo* assays where p38 was inhibited showed decreased SRC-3 phosphorylation at S857. Conversely, stimulation of p38 with the stress-activator anisomycin increased the phosphorylation more than 2-fold. This demonstrates that p38 could be a possible indirect upstream kinase of SRC-3 phosphorylation of S857 (through MK2). The *in vivo* assays were repeated with corresponding results, but more parallels are needed to statistically confirm our results. However, we have demonstrated that of the MAPKs, p38 is the most likely MAP kinase to be the upstream of SRC-3 phosphorylation at S857 in H1299 cells.

The p38pathway as a possible upstream regulator of SRC-3

As illustrated in Figure 18, the p38 MAP kinase could be a possible regulator of SRC-3 through its activation of MK2 (a MAPKAP kinase). The latter is the kinase which directly mediates the phosphorylation of SRC-3 at S857. It is evident that further studies are required in order to strengthen this theory. One way to address this could be by using MK2 deficient mice cells.

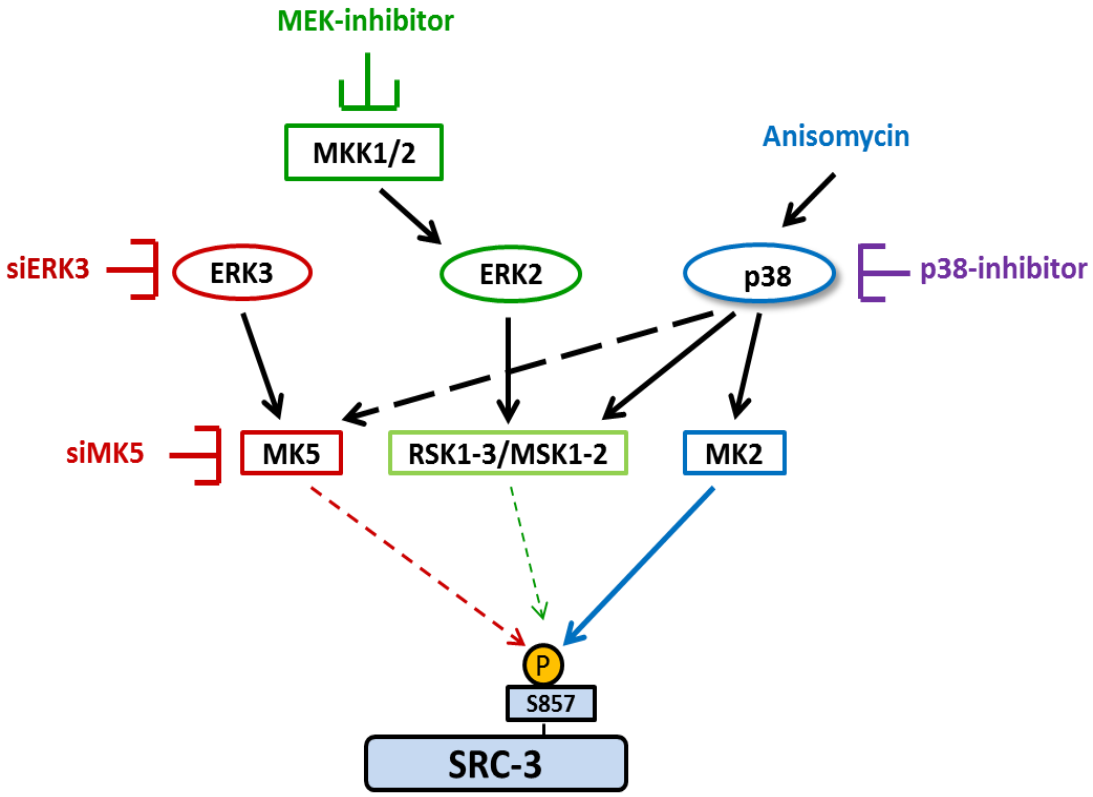

Figure 18: Illustration of pathways investigated *in vitro* and *in vivo* for phosphorylation of SRC-3 at S857. MK5 phosphorylates SRC-3 at S857 efficiently *in vitro*. Conversely, siRNA mediated knockdown of ERK3 and MK5 failed to prove this pathway to be involved in phosphorylation *in vivo* (red color). ERK2 did not phosphorylate SRC-3 at S857 efficiently neither *in vitro* nor *in vivo* (green color).The p38 MAPK did not phosphorylate SRC-3 at S857 efficiently *in* vitro, but stimulation of p38 with the stress-activator anisomycin increased the phosphorylation more than 2-fold *in vivo* (blue color). By using the p-38 inhibitor SB-202190 (purple), the levels of phosphorylation *in vivo* decreased. MK2, a downstream target of p38, phosphorylate SRC-3 at S857 efficiently *in vitro*. Taken together, our results indicate the p38 pathway to be involved in SRC-3 phosphorylation at S857. siERK3 and siMK5 indicates siRNA mediated knockdown of ERK3 and MK5, respectively.

In 2004, Wu et al reported the SRC-3 residue S857 to be phosphorylated by the IκB kinase (IKK), but not by p38 MAPK (44). They hypothesized that different phosphorylated forms of SRC-3 are utilized by distinct signaling pathways to exert distinct physiological responses. Their siRNA assays resulted in the identification of S505, S543, S860 and S867, and not S857, as residues phosphorylated by the p38 MAP kinase. This is in contrast to our results, which suggest that the p38 MAPK signaling pathway can mediate phosphorylation of the S857 residue through its downstream effector MK2 or MK3. This association has not been reported earlier. In fact, no MAPKAPKs have been suggested to phosphorylate S857 or any other site of SRC-3 before.

The residues S857, S860 and S867 are unique and amongst the SRC-family are found only in SRC-3, and they all reside in the CBP-interaction domain (CID) of SRC-3. Interestingly, Wu et al tested knockdown of p38 and found it not to affect SRC-3 phosphorylation at S857. These experiments should be repeated using various cell lines to further study the association of the p38 MAPK and the SRC-3 residue S857.

The fact that SRC-3 is a transcriptional co-activator for the transcription factor NF-κB, which is activated by stress stimuli, also implies that the p38 pathway could be upstream of SRC-3.

7 CONCLUSION/FUTURE PERSPECTIVES

Much more work is required to further investigate our findings that the p38 pathway is involved in the phosphorylation of SRC-3 at S857 both *in vitro* and *in vivo*. This could be addressed by using knockout mice that lack the expression of MK2. Elucidation of upstream regulators of SRC-3 will increase our understanding of the molecular aspects of SRC-3 phosphorylation. This will enable us to take advantage of this knowledge in the development of novel cancer therapeutics that could hopefully prove to be beneficial for various groups of cancer patients. For this reason, our observations could be of clinical importance.

REFERENCES

1. Schenk PW, Snaar-Jagalska BE. Signal perception and transduction: the role of protein kinases. Biochim Biophys Acta. 1999;1449(1):1-24.
2. Manning G, Whyte DB, Martinez R, Hunter T, Sudarsanam S. The protein kinase complement of the human genome. Science. 2002;298(5600):1912-34.
3. Blume-Jensen P, Hunter T. Oncogenic kinase signalling. Nature. 2001;411(6835):355-65.
4. Cohen P. The regulation of protein function by multisite phosphorylation--a 25 year update. Trends Biochem Sci. 2000;25(12):596-601.
5. Schlessinger J. Cell signaling by receptor tyrosine kinases. Cell. 2000;103(2):211-25.
6. Kolibaba KS, Druker BJ. Protein tyrosine kinases and cancer. Biochim Biophys Acta. 1997;1333(3):F217-48.
7. Lemmon MA, Schlessinger J. Cell signaling by receptor tyrosine kinases. Cell. 2010;141(7):1117-34.
8. Pawson T, Nash P. Protein-protein interactions define specificity in signal transduction. Genes Dev. 2000;14(9):1027-47.
9. Cohen P. Protein kinases--the major drug targets of the twenty-first century? Nature reviews Drug discovery. 2002;1(4):309-15.
10. Gschwind A, Fischer OM, Ullrich A. The discovery of receptor tyrosine kinases: targets for cancer therapy. Nat Rev Cancer. 2004;4(5):361-70.
11. Coulombe P, Meloche S. Atypical mitogen-activated protein kinases: Structure, regulation and functions. Biochimica et Biophysica Acta (BBA) - Molecular Cell Research. 2007;1773(8):1376-87.
12. Dhanasekaran DN, Johnson GL. MAPKs: function, regulation, role in cancer and therapeutic targeting. Oncogene. 0000;26(22):3097-9.
13. Kostenko S, Dumitriu G, Moens U. Tumour promoting and suppressing roles of the atypical MAP kinase signalling pathway ERK3/4-MK5. Journal of molecular signaling. 2012;7(1):9.
14. Davis RJ. The mitogen-activated protein kinase signal transduction pathway. J Biol Chem. 1993;268(20):14553-6.
15. Seternes O-M, Mikalsen T, Johansen B, Michaelsen E, Armstrong CG, Morrice NA, et al. Activation of MK5/PRAK by the atypical MAP kinase ERK3 defines a novel signal transduction pathway. EMBO J. 2004;23(24):4780-91.
16. Drew BA, Burow ME, Beckman BS. MEK5/ERK5 pathway: the first fifteen years. Biochim Biophys Acta. 2012;1825(1):37-48.
17. Chen Z, Gibson TB, Robinson F, Silvestro L, Pearson G, Xu B, et al. MAP kinases. Chem Rev. 2001;101(8):2449-76.
18. Roux PP, Blenis J. ERK and p38 MAPK-activated protein kinases: a family of protein kinases with diverse biological functions. Microbiol Mol Biol Rev. 2004;68(2):320-44.
19. Kohno M, Pouyssegur J. Targeting the ERK signaling pathway in cancer therapy. Ann Med. 2006;38(3):200-11.
20. Johnson GL, Lapadat R. Mitogen-activated protein kinase pathways mediated by ERK, JNK, and p38 protein kinases. Science. 2002;298(5600):1911-2.
21. Raman M, Chen W, Cobb MH. Differential regulation and properties of MAPKs. Oncogene. 2007;26(22):3100-12.
22. Nithianandarajah-Jones GN, Wilm B, Goldring CE, Muller J, Cross MJ. ERK5: structure, regulation and function. Cell Signal. 2012;24(11):2187-96.
23. Lochhead PA, Gilley R, Cook SJ. ERK5 and its role in tumour development. Biochem Soc Trans. 2012;40(1):251-6.
24. Dhillon AS, Hagan S, Rath O, Kolch W. MAP kinase signalling pathways in cancer. Oncogene. 2007;26(22):3279-90.

25. Weston CR, Davis RJ. The JNK signal transduction pathway. Curr Opin Cell Biol. 2007;19(2):142-9.
26. Johnson GL, Nakamura K. The c-jun kinase/stress-activated pathway: regulation, function and role in human disease. Biochim Biophys Acta. 2007;1773(8):1341-8.
27. Lee JC, Laydon JT, McDonnell PC, Gallagher TF, Kumar S, Green D, et al. A protein kinase involved in the regulation of inflammatory cytokine biosynthesis. Nature. 1994;372(6508):739-46.
28. Cuenda A, Rousseau S. p38 MAP-kinases pathway regulation, function and role in human diseases. Biochim Biophys Acta. 2007;1773(8):1358-75.
29. del Barco Barrantes I, Nebreda AR. Roles of p38 MAPKs in invasion and metastasis. Biochem Soc Trans. 2012;40(1):79-84.
30. Åberg E, Torgersen KM, Johansen B, Keyse SM, Perander M, Seternes O-M. Docking of PRAK/MK5 to the Atypical MAPKs ERK3 and ERK4 Defines a Novel MAPK Interaction Motif. J Biol Chem. 2009;284(29):19392-401.
31. Åberg E, Perander M, Johansen B, Julien C, Meloche S, Keyse SM, et al. Regulation of MAPK-activated Protein Kinase 5 Activity and Subcellular Localization by the Atypical MAPK ERK4/MAPK4. J Biol Chem. 2006;281(46):35499-510.
32. Perander M, Keyse SM, Seternes OM. Does MK5 reconcile classical and atypical MAP kinases? Front Biosci. 2008;13:4617-24.
33. Abe MK, Kuo WL, Hershenson MB, Rosner MR. Extracellular signal-regulated kinase 7 (ERK7), a novel ERK with a C-terminal domain that regulates its activity, its cellular localization, and cell growth. Mol Cell Biol. 1999;19(2):1301-12.
34. Henrich LM, Smith JA, Kitt D, Errington TM, Nguyen B, Traish AM, et al. Extracellular signal-regulated kinase 7, a regulator of hormone-dependent estrogen receptor destruction. Mol Cell Biol. 2003;23(17):5979-88.
35. Cargnello M, Roux PP. Activation and function of the MAPKs and their substrates, the MAPK-activated protein kinases. Microbiol Mol Biol Rev. 2011;75(1):50-83.
36. Gaestel M. MAPKAP kinases — MKs — two's company, three's a crowd. Nat Rev Mol Cell Biol. 2006;7(2):120-30.
37. Robinson-White A, Stratakis CA. Protein kinase A signaling: "cross-talk" with other pathways in endocrine cells. Ann N Y Acad Sci. 2002;968:256-70.
38. Steroid receptor coactivator-3 as a potential molecular target for cancer therapy. Expert Opin Ther Targets. 2012;16(11):1085-96.
39. Ma G, Ren Y, Wang K, He J. SRC-3 has a role in cancer other than as a nuclear receptor coactivator. Int J Biol Sci. 2011;7(5):664-72.
40. York B, O'Malley BW. Steroid Receptor Coactivator (SRC) Family: Masters of Systems Biology. J Biol Chem. 2010;285(50):38743-50.
41. Lonard DM, O'Malley BW. Nuclear receptor coregulators: modulators of pathology and therapeutic targets. Nat Rev Endocrinol. 2012;8(10):598-604.
42. Yan J, Tsai SY, Tsai M-j. SRC-3/AIB1: transcriptional coactivator in oncogenesis. Acta Pharmacol Sin. 2006;27(4):387-94.
43. Long W, Foulds CE, Qin J, Liu J, Ding C, Lonard DM, et al. ERK3 signals through SRC-3 coactivator to promote human lung cancer cell invasion. The Journal of Clinical Investigation. 2012;122(5):1869-80.
44. Wu RC, Qin J, Yi P, Wong J, Tsai SY, Tsai MJ, et al. Selective phosphorylations of the SRC-3/AIB1 coactivator integrate genomic reponses to multiple cellular signaling pathways. Mol Cell. 2004;15(6):937-49.
45. Gojis O, Rudraraju B, Gudi M, Hogben K, Sousha S, Coombes CR, et al. The role of SRC-3 in human breast cancer. Nat Rev Clin Oncol. 2010;7(2):83-9.
46. Cai D, Shames DS, Raso MG, Xie Y, Kim YH, Pollack JR, et al. Steroid Receptor Coactivator-3 Expression in Lung Cancer and Its Role in the Regulation of Cancer Cell Survival and Proliferation. Cancer Res. 2010;70(16):6477-85.

47. Wang Y, Lonard DM, Yu Y, Chow D-C, Palzkill TG, O'Malley BW. Small Molecule Inhibition of the Steroid Receptor Coactivators, SRC-3 and SRC-1. Mol Endocrinol. 2011;25(12):2041-53.
48. Wang Y, Lonard DM, Yu Y, Chow D-C, Palzkill TG, Wang J, et al. Bufalin is a potent small molecule inhibitor of the steroid receptor coactivators SRC-3 and SRC-1. Cancer Res. 2014.
49. Davies SP, Reddy H, Caivano M, Cohen P. Specificity and mechanism of action of some commonly used protein kinase inhibitors. Biochem J. 2000;351(Pt 1):95-105.

APPENDIX

Appendix 1: Kinase assays

Kinase[1] (ng)	GST-SRC-3 (µl)	Kinase buffer (µl)	Milli-Q H_2O (µl)	Total volume (µl)	2 x LDS buffer (µl)	Sample Reducing Agent (µl)
100	10	50	X	100	20	4
5	5	25	X	50	50	10
10	5	25	X	50	50	10
20	5	25	X	50	50	10
40	5	25	X	50	50	10

[1] **Each kinase reaction was incubated at 30 °C for 5, 10, 15 and 30 minutes.**

Appendix 2: Phosphorylation of CID SRC-3 at S857 by 5-40 ng MK5

Amount of MK5 (ng)	Quantitative value
5	1.49
10	3.18
20	8.32
40	11.08

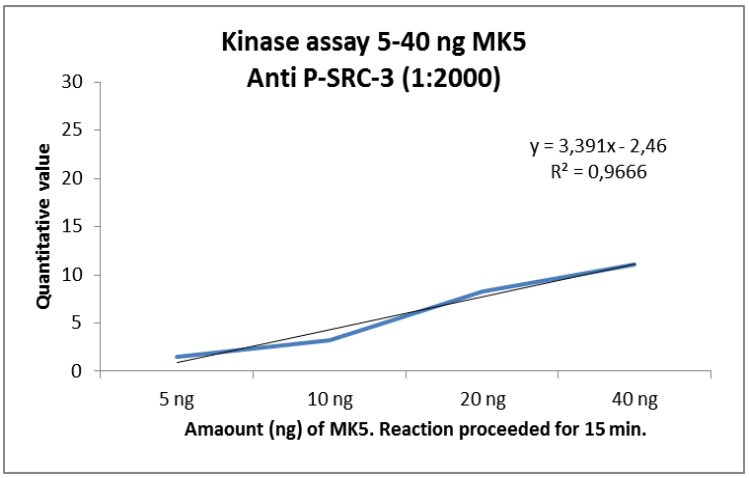

Appendix 3: Phosphorylation of CID SRC-3 at S857 by 100 ng MK5

Time (min) of incubation of kinase reaction	Quantitative value
5	31.64
10	34.43
15	41.34
30	46.43

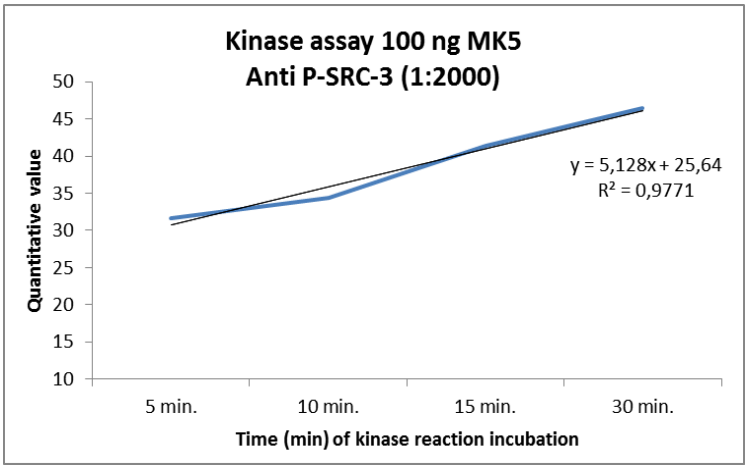

Appendix 4: Phosphorylation of CID SRC-3 at S857 by 5-40 ng MK2

Amount of MK5 (ng)	Quantitative value
5	5.03
10	9.49
20	20.13
40	26.03

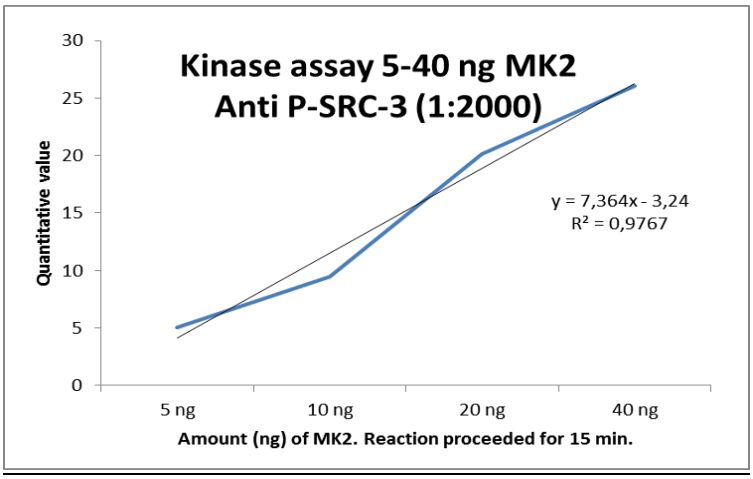

Appendix 5: Phosphorylation of CID SRC-3 at S857 by 100 ng MK2

Time (min) of incubation of kinase reaction	Quantitative value
5	16.01
10	23.54
15	24.34
30	27.47

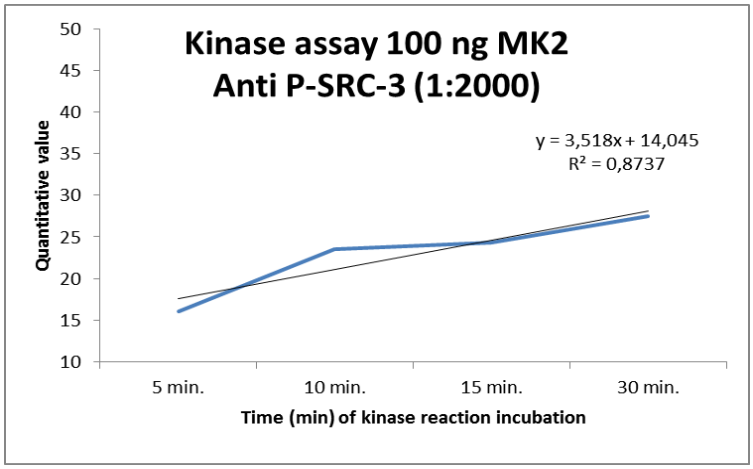

Appendix 6: Quantitative analysis of SRC-3 S857 phosphorylation

Lysate	Quantitative value P-S857 SRC-3[a]	Quantitative value total SRC-3[b]	Proportion P-S857 SRC-3 of total SRC-3[c (a/b)]	Proportion of P-S857 SRC-3 compared to control
DMSO[1]	0,17	0,83	0,204819277	
MEK-inhibitor[2]	0,18	0,5	0,360000000	1,76[2c/1c]
P38-inhibitor[3]	0,02	0,76	0,026315789	0,13[3c/1c]
Control siRNA[4]	0,33	2,16	0,152777778	
siRNA MK5[5]	0,19	1,2	0,158333333	1,04[5c/4c]
siRNA ERK3[6]	0,34	1,9	0,178947368	1,17[6c/4c]
Untreated[7]	0,06	0,31	0,193548387	
Anisomycin[8]	0,3	0,69	0,434782609	2,25[8c/7c]
DMSO[9]	0,22	0,22	0,019064125	
PKA-inhibitor[10]	11,54	11,30	0,019469027	1,02[10c/9c]

<u>Appendix 7:</u> SeeBlue® Plus2 Pre-Stained Protein Standard 1x

Invitrogen, Life Technologies™ (**<u>www.lifetechnologies.com</u>**)